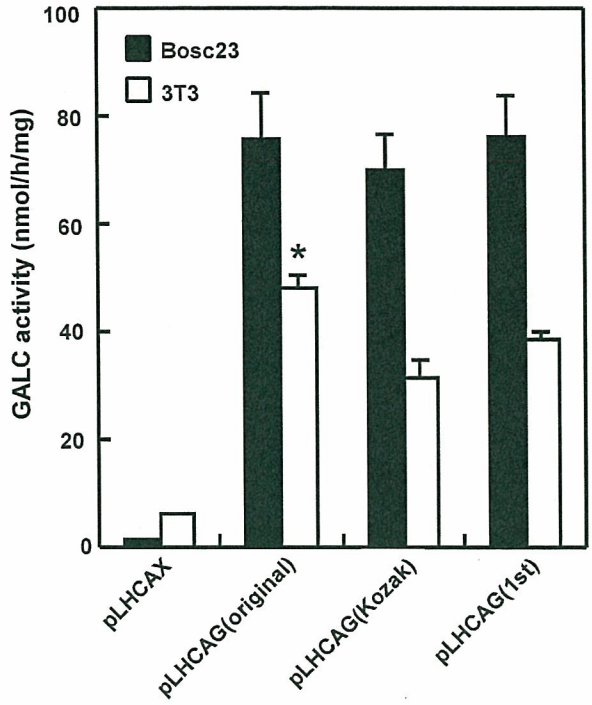

Fig. 2. Influence of ATG surrounding sequence to GALC activity. GALC activities in Bosc23 ($n = 6$) and NIH/3T3 ($n = 3$) cells transfected with retroviral vectors carrying GALC cDNA with "original ATG", "Kozak ATG" or "1st ATG." pLHCAX was used as control vector. The data are presented as mean ± SE *$P = 0.015$ and 0.038, ("original ATG" compared with "Kozak ATG" and "1st ATG" respectively, t test).

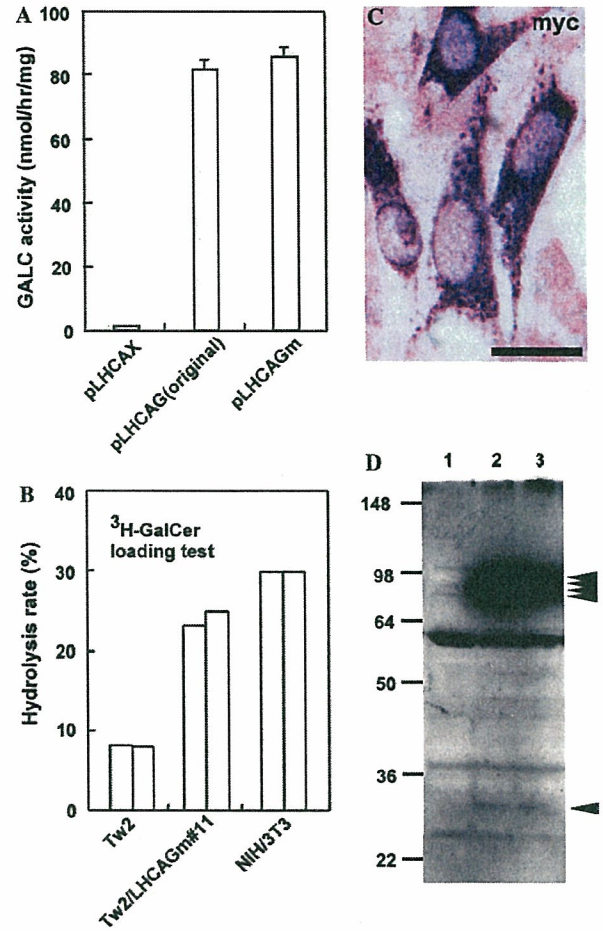

Fig. 3. Characterization of epitope tagged GALC protein. (A) GALC activities in Bosc23 ($n = 3$) transfected with retroviral vectors carrying GALC with (pLHCAGm) or without myc-tag (pLHCAG). pLHCAX was used as control vector. The data are presented as mean ± SE. (B) Hydrolysis rates of GalCer in twitcher fibroblasts (Tw2), a subclone of retrovirus LHCAGm-infected Tw2 (Tw2/LHCAGm#11) and NIH/3T3, assessed by [^{3}H]GalCer loading test ($n = 2$). (C) Myc-tag-immunocytochemistry in a subclone of ψMP34 stably transduced with pLHCAGm (ψMP34/pLHCAGm#92). Parental ψMP34 is a mouse fibroblasts-derived packaging cell line. (D) Western blot analysis of cell extracts from parental cell line ψMP34 (lane 1) and two subclones of ψMP34 stably transduced with pLHCAGm (ψMP34/pLHCAGm#92 and #96; lanes 2 and 3, respectively) labeled with rabbit antibody to the myc-tag. The molecular weight standards are shown on the left. Transgene-specific bands are indicated by arrowheads.

of tag, so the construct encoding GALC with triple epitope-tag (named as pLHCAGm, Fig. 1) was used subsequently to produce recombinant retrovirus.

It is critical to determine whether epitope-tag interferes with the normal structure and biological activity of GALC protein. Transient expression study showed that no decrement of GALC activity in the cells transfected with pLHCAGm comparing with the parent construct without epitope tagging (Fig. 3A). To further confirm that epitope tagging has no adverse effects on GALC, [^{3}H]GalCer loading test was carried out on a subclone of twitcher fibroblasts expressing myc-tagged-GALC (Tw2/LHCAGm#11;GALC activity: 14.07 nmol/h/mg). The hydrolysis rate of GalCer in Tw2/LHCAGm#11 significantly increased as compared with uninfected parental twitcher fibroblasts (Tw2), near that in NIH/3T3 cells (Fig. 3B). This demonstrated that GALC deficiency in the twitcher cells was restored by LHCAGm transduction and that epitope tagging has no influence on lysosomal targeting and intracellular catalytic activity of recombinant GALC protein.

Immunocytochemistry using antibody against myc-tag in cells stably transduced with pLHCAGm showed punctated stains throughout the cytoplasm (Fig. 3C). Western blot analysis of cell extracts from these cells showed transgene-specific bands between 80 and 90 kDa (four bands could be identified in shorter time of exposure) and one at about 30 kDa (Fig. 3D, arrowheads). The bands of 80–90 kDa may present the precursor form of GALC and the band near 30 kDa may present the C-terminal subunit of GALC [31–33]. The signal strength in 80–90 kDa was significantly stronger than that in 30 kDa suggesting that most of the immunoreactive signals observed in the immunocytochemical study above may be contributed to the precursor form of GALC protein.

Stable gene transfer to oligodendrocytes by SVZ injection of retrovirus

To transduce oligodendrocytes in vivo, we introduced retrovirus into the SVZ at neonatal period in the mouse. To investigate the pattern of gene transfer by SVZ injection, LHCAL was injected stereotactically into the SVZ of neonatal normal mice and the transduction pattern was examined by X-gal histochemistry and immunohistochemistry at P4 and P30. No noticeable inflammatory and other abnormality was observed in the brain. At P4, many β-gal$^+$ cells still remained in the SVZ and some positive cells were observed in the cortex and the white matter dorsal or lateral to the SVZ (Fig. 4A). At P30, when migration and differentiation of neural cells are almost completed in the mouse brain, β-gal$^+$ cells were scattered widely in the neocortex, subcortical white matter, and the striatum of the ipsilateral hemisphere (Fig. 4B). Few positive cells could be seen in the contralateral hemisphere. All transduced cells appeared to be glia and most of them could be classified into oligodendrocytes and astrocytes by morphological criteria described previously [26]. No β-gal$^+$ neuron could be found. Transduced oligodendrocytes were distributed both in the gray and white matter. In the white matter β-gal$^+$ oligodendrocytes had many longitudinal processes parallel to nerve fiber tract presumably the cytoplasmic tongues of myelin sheaths (Fig. 4C), while many transduced oligodendrocytes in the cerebral cortex showed abundant, tenuous processes corresponding to type I oligodendrocytes [34] (Fig. 4D). Most transduced astrocytes have protoplasmic morphology with highly branched feather-like processes (Fig. 4E). Cell type identification was further confirmed by double immunofluorescence using antibodies to both β-gal and cell type-specific markers (GFAP for astrocytes, GST-π and MBP for oligodendrocytes) (Figs. 4F and G).

The results were essentially consistent with earlier studies in rats [26] and demonstrated that SVZ injection of retrovirus in neonatal mouse is an ideal strategy to achieve persistent transduction of oligodendrocytes from early developmental stages.

Transduction of GALC to twitcher brain

GALC-expressing retrovirus LHCAGm was injected into the SVZ of twitcher mice at P0. Two out of 10 recipients disappeared at the next day and eight recipients survived at the time of analysis. No changes in the clinical symptoms such as small body, twitching and paralysis of hind limbs were observed in the LHCAGm injected twitcher mice comparing with untreated twitcher controls.

At P38–40, LHCAGm injected twitcher brains were studied for transgene expressing-cells by immunohistochemistry against myc-tag. Myc$^+$ cells were identified in four out of five examined twitcher brains. The distribution pattern of myc$^+$ cells in the brain sections was similar to that of β-gal$^+$ cells observed in the LHCAL injected normal mice described above. The number of myc$^+$ cells in the twitcher brain varies slightly among animals with an average number of ~10 cells in the cerebral cortex per section. All myc$^+$ cells were glial cells and most of them could be defined as either oligodendrocytes or astrocytes by their morphology. The transduced

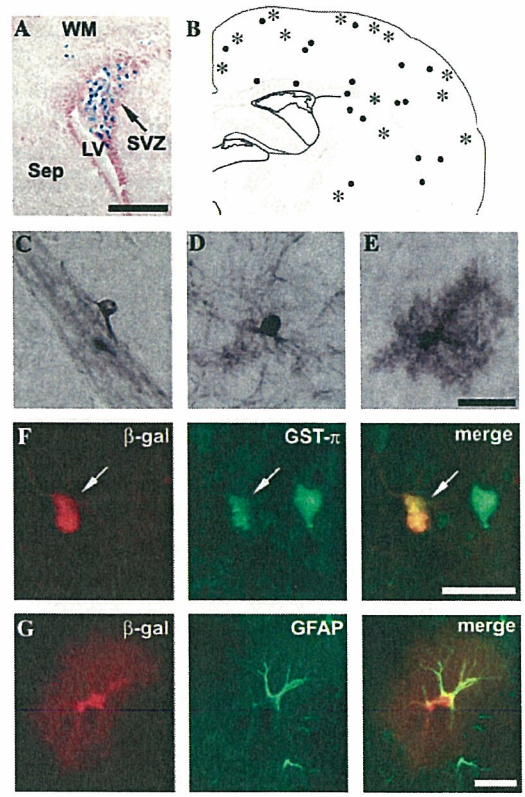

Fig. 4. Gene transfer to the brain of normal mouse by SVZ injection of LHCAL. (A) X-gal stained coronal brain section at P4 shows many β-gal$^+$ cells (blue) located in the SVZ. The level of the section nears the site of injection. (B) Schematic representation of the distribution of β-gal$^+$ cells based on immunostaining to β-gal in the recipient's brain at P30. Closed circles and asterisks represent positive oligodendrocytes and astrocytes respectively. (C–E) Microscopic photographs of β-gal-immunoreactive glial cells in the recipients brain at P30. (C) A positive oligodendrocyte in the white matter. Note immunoreactive longitudinal processes parallel to the nerve tract. (D) An immunoreactive oligodendrocyte in the cerebral cortex. (E) A positive protoplasmic astrocyte in the cerebral cortex. (F and G) Cell-type identification of transduced cells by double immunofluorescence. (F) A β-gal-immunoreactive cell (red) in the cerebral cortex was GST-π$^+$ (green), indicating it is an oligodendrocyte. (G) Two β-gal-immunoreactive cells (red) in the cerebral cortex were GFAP$^+$ (green), indicating they are astrocytes. The two cells contact closely suggesting they may be daughters of the same progenitor. LV, lateral ventricle; WM, white matter; Sep, septum; SVZ, subventricular zone. The schema of the brain in (B) was adopted from "Brain Maps: Structure of the rat Brain" by Swanson [30]. Scale bar: 250 μm in (A); 25 μm in (C–E); 20 μm in (F and G). (For interpretation of the references to colors in this figure legend, the reader is referred to the web version of this paper.)

oligodendrocytes exhibited an intense cytoplasmic staining with moderately stained asymmetrical nucleus (Fig. 6E). Only a few proximal processes extended from cell body could be identified in LHCAGm transduced oligodendrocytes. Myc$^+$ astrocytes exhibited stains in the rim of cytoplasm and abundant bushy processes with relatively pale nucleus (Fig. 6F).

The presence and expression of transduced GALC gene in the recipient twitcher brain was analyzed by PCR and RT-PCR using primers specific for human GALC at P35–39 (Fig. 5). All three twitcher recipients' brains examined were positive for human GALC cDNA (provirus DNA) and human GALC transcript. The authenticity of the PCR product was confirmed by Southern blot with a human GALC probe. GALC expression was further assessed by enzymatic assay. There was no measurable GALC activities in the transduced twitcher brain above untreated twitcher controls (GALC activities: 0.05 ± 0.01, 0.08 ± 0.01, and 2.24 ± 0.14 nmol/h/mg in transduced twitcher, age-matched untreated twitcher and untreated normal mouse brain, respectively, each three animals). This was not unexpected since the number of transduced cells in the brain was very small. The activity of transduced GALC in the whole brain homogenate may be under the detection limit of this enzyme assay system.

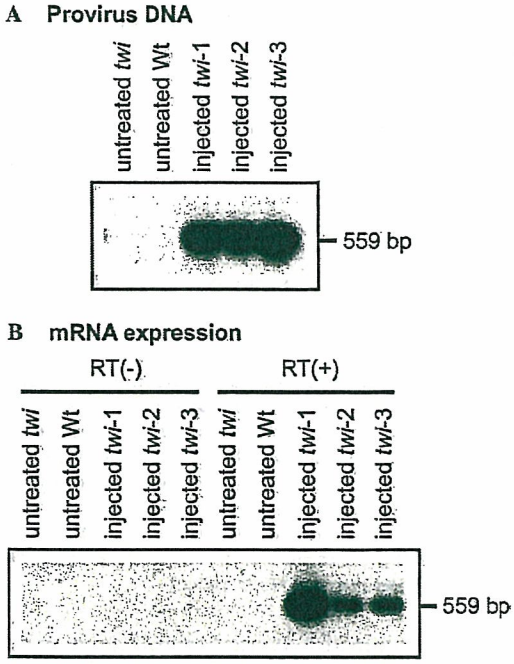

Fig. 5. Presence and expression of transduced human GALC in the twitcher brains which received neonatal SVZ injection of LHCAGm. Southern blot analysis. (A) PCR amplification of genomic DNA from the whole brain to detect the presence of the integrated provirus. (B) Human GALC transcript was detected by RT-PCR using total RNA from the whole brain. The authenticity of PCR products was confirmed by hybridized with a human GALC probe. RT (+) and RT (−) indicate amplified PCR products form cDNA samples with and without reverse transcriptase, respectively.

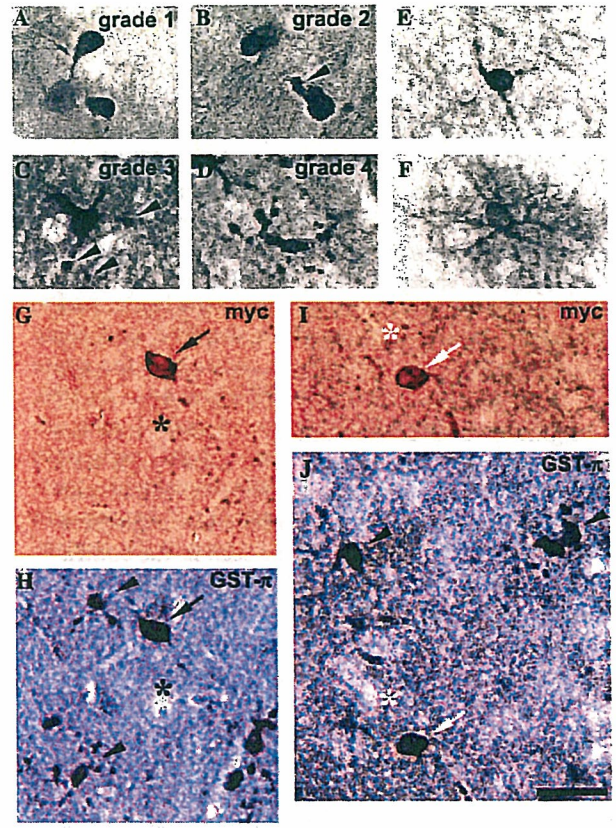

Fig. 6. Morphological correction of twitcher oligodendrocytes by GALC transduction. (A–D) The severity of morphological aberrations of oligodendrocytes in the cerebral cortex was divided into four grades by GST-π-immunostaining. (E and F) LHCAGm transduced oligodendrocyte (E) and astrocyte (F) in the twitcher cerebral cortex at around P40, identified by immunohistochemistry against myc-tag. (G and H) A representative brain section from LHCAGm injected twitcher cerebral cortex subsequently stained with mouse anti-myc-tag (G, chromogen: AEC) and rabbit anti-GST-π (H, chromogen: DAB-$NiCl_2$) antibodies. A myc$^+$/GST-π$^+$ cell (arrow) exhibits normal morphology (Grade 1), while myc$^-$/GST-π$^+$ cells (arrowheads) show severe aberrant morphologies (Grades 3 and 4). Asterisk indicates the blood vessel nearing myc$^+$ cell as anatomic marker. (I and J) Another brain section stained with anti-myc (I) and anti-GST-π (J) antibodies. Scale bar: 20 μm.

Morphological improvements in GALC transduced oligodendrocytes in the twitcher brain

To evaluate the effects of GALC transduction on the morphology of oligodendrocytes, an analysis using combined immunostaining for myc-epitope and GST-π was carried out. GST-π has been well documented as a marker of oligodendrocytes [35] and previously used to investigate morphological aberrations in twitcher oligodendrocytes [8]. Unlike many other oligodendroglial markers such as MBP, 2′,3′-cyclic nucleotide

3′-phosphodiesterase (CNPase), and proteolipid protein (PLP) that mainly stain the processes of oligodendrocytes and myelin, GST-π clearly reveals the cell soma and some processes and appears suitable for morphological investigation of oligodendrocytes.

Oligodendroglial morphology was examined in the cerebral cortex since unlike those in the white matter oligodendrocytes in the cerebral cortex is less compact distributed which makes the morphological examination much easier to perform. To quantitatively evaluate the aberrations in the morphology of oligodendrocytes, the severity of morphological changes were divided to four grades based on their morphologies in the normal and untreated twitcher mice at P40 after GST-π-immunostaining: Grade 1, spherical, oval or slightly polygonal soma (Fig. 6A). This is typical normal morphology and almost all oligodendrocytes in the normal mouse show this morphology. Grade 2, slightly polygonal soma with one or two swelling-like structures (Fig. 6B, arrowhead) at the soma or the proximal processes. This morphology may be abnormal but could also be seen in oligodendrocytes of the normal mouse at low frequency, so it represents normal or slightly abnormal morphology. Grade 3, markedly altered morphology including enlarged soma, irregularly thick processes and various sizes of swellings at different sites of the processes (Fig. 6C, arrowheads). The morphologies of this grade are never seen in oligodendrocytes of the normal mouse, while most oligodendrocytes in the twitcher at P40 show these morphologies. Grade 4, severe aberrant morphology with shrunken soma and/or fragmented processes (Fig. 6D). Oligodendrocytes displaying this morphology probably correspond to the apoptotic oligodendrocytes described previously [8].

The summary of morphological analysis of oligodendrocytes was shown in Table 1. Around P40, more than 93% of the cerebral cortical oligodendrocytes (GST-π^+ cells) in the untreated twitcher mice showed severe aberrant morphologies (Grade 3–4) (Figs. 6C and D). As viral infection controls, neonatal twitcher mice received LHCAL injection were analyzed for morphologies of transduced oligodendrocytes (β-gal$^+$/GST-π^+ cells) at P38–39. More than 86% β-gal$^+$/GST-π^+ cells in these mice had severe abnormal morphology (Grade 3–4). This suggests that virus vector injection itself does not alter the morphology of oligodendrocytes in the twitcher mice.

In contrast, dramatic morphological improvement in oligodendrocytes was observed in the twitcher mice that received LHCAGm. About 83% of GALC expressing-oligodendrocytes (myc$^+$/GST-π^+ cells) exhibited completely normal morphology (Grade 1) (arrows in Figs. 6G–J). Only less than 5% of myc$^+$/GST-π^+ cells had typical abnormal morphology such as swellings at the soma or processes (Grade 3). And none was classified to Grade 4. The percentages of cells of each grade within myc$^+$/GST-π^+ cells in these mice were significantly different from that in untreated twitcher mice or twitcher mice received LHCAL injection ($P < 0.0001$, χ^2 test). Despite the significant normalization of myc$^+$ oligodendrocytes in LHCAGm transduced twitcher mice, the untransduced (myc-negative) oligodendrocytes located nearing showed aberrations in morphology (arrowheads in Figs. 6H and J). When morphological analysis was performed on GST-π^+ cells in the cerebral cortex of these mice regardless of myc-immunoreactivity, the percentages of cells of each grade were undistinguishable from those in untreated twitcher controls. This indicates that the persistent expression of GALC in a small number of glial cells did not result in diffuse correction of neighboring oligodendrocytes in the twitcher brain.

Discussion

At present hematopoietic stem cell transplantation is the only available treatment for GLD, especially the late-onset form [4]. At the mean time, gene therapy is another promising strategy to treat inherited disorders like GLD which results from mutations of a single gene. Basic studies on the understanding of the effects of transduced GALC in myelin-forming cells are important in the assessment of the potential of gene therapy in GLD. Previous experiments that introduced GALC gene into cultured oligodendrocytes derived from twitcher showed appropriate localization of the enzyme and normal morphology with highly branched processes in some transduced oligodendrocytes [16,17]. In the present study, an in vivo model for transducing oligodendro-

Table 1
Morphological analysis of oligodendrocytes in the cerebral cortex

Morphological grading	Wild type	Untreated twitcher	Twitcher-LHCAL	Twitcher-LHCAGm	
	GST-π^+ ($n=3$)	GST-π^+ ($n=4$)	β-gal$^+$/GST-π^+ ($n=3$)	myc$^+$/GST-π^+ ($n=4$)	GST-π^+ ($n=3$)
1	99.6 ± 0.3% (3281)	1.8 ± 0.3% (28)	5.3 ± 1.9% (10)	83.5 ± 1.3% (101)	1.0 ± 0.3% (19)
2	0.4 ± 0.3% (14)	4.4 ± 1.2% (69)	8.6 ± 1.2% (19)	11.9 ± 1.2% (15)	3.2 ± 0.9% (60)
3	0% (0)	85.8 ± 1.5% (1385)	73.8 ± 0.8% (160)	4.6 ± 1.2% (5)	87.8 ± 1.1% (1708)
4	0% (0)	8.1 ± 1.3% (132)	12.3 ± 1.3% (28)	0% (0)	8.0 ± 1.3% (154)
Total	100% (3295)	100% (1614)	100% (217)	100% (121)	100% (1941)

Data is presented as mean ± SE. In parentheses are the sums of cell numbers counted from 3 or 4 animals.

cytes with GALC was developed and results showed that the morphology was completely corrected in most of the transduced twitcher oligodendrocytes. This suggested that GALC may play an important role in the maintenance of the normal morphology of oligodendrocytes in vivo and provided direct evidence for the usefulness of gene therapy in GLD.

It is known that many lysosomal enzymes can be secreted from normal cells and taken up by enzyme-deficient cells, and this process, called cross-correction, occurs either by direct cell-to-cell transfer or cell surface receptor-mediated endocytosis. Cross-correction is an important concept in gene therapy strategies to treat lysosomal storage diseases since the non-transduced affected cells could also be corrected by this mechanism. And it is also the rationale for the use of hematopoietic stem cell or intracerebral cell transplantation in treating lysosomal diseases that affects the CNS such as Krabbe disease. Previous studies demonstrated that GALC can be secreted into culture medium from normal or over-expressing cells and can be incorporated by several types of enzyme-deficient cells including oligodendrocytes, astrocytes and Schwann cells in vitro [17,36,37]. In the present study, we initially expected that positive signal could be detected in the neural cells neighboring the transduced cells. However, the myc-tag-immunostaining in the brain always showed sharp boundaries between positive and negative cells and we could not observe traces of immunoreactive signals in the brain cells neighbor, even adjacent to positive glial cells above background (Figs. 6G and I). Moreover, despite of the significant morphological correction of myc$^+$ twitcher oligodendrocytes, we could not observe phenotypic changes in oligodendrocytes located nearing positive oligodendrocytes (e.g., the cell on the left upper hand of Fig. 6H pointed by arrowhead). Thus we did not obtain histological evidence for cross-correction of GALC in vivo. However, we cannot rule out the possibility that the level of GALC expression in vivo in our study was relatively low and the amount of enzyme supplied to surrounding cells was insufficient to achieve morphological restoration or to be detected by the immunostaining. Another possible reason could be that the cross-correction process of human GALC is insufficient in the mouse cells. For this, a specifically designed study should be needed to determine the evidence and implications of cross-correction of GALC in vivo.

Stable transduction of oligodendrocytes is essential for successful examination of the in vivo effects of the transgene. To transduce oligodendrocytes, we chose SVZ injection of retrovirus at neonatal period. This is because that in murine, gliogenesis takes place largely in early postnatal life and most oligodendroglial progenitor cells are located in the SVZ at neonatal period. These mitotically active progenitor cells could be infected by retrovirus, migrate away from the SVZ and differentiate into mature oligodendrocytes. Results showed that the neonatal injection of retrovirus into SVZ has significant advantages over direct injection of viral vectors into brain parenchyma to transduce mature oligodendrocytes. The latter usually transduces various types of cells concentrated at the injection sites and leads to obvious trauma and inflammatory reactions making the morphological analysis difficult to perform. Comparing with the infectious titer of LHCAGm the transduction level in this study was low (up to 10 myc$^+$ cells were observed in the cerebral cortex per section). The presence of inhibitory factors (non-transducing viral particles and free viral envelope proteins) in the viral stocks may be one of the reasons for the discrepancy between the low in vivo transfectability and the viral titer [38].

Sensitive localization of the protein products of transgene in vivo is an important issue in evaluating the effects of the transgene. Although polyclonal antibodies against GALC have been used to identify GALC-expressing cells in culture systems and tissues previously [17,39], our results showed epitope tagging is also useful. Immunohistochemistry using commercially available antibodies to myc-tag gave to sensitive detection of transduced GALC with satisfactory signal-to-noise ratio in the brain tissues. Epitope-tags at the C-terminus of GALC protein did not interfere with lysosomal targeting and the bioactivity of transduced GALC as demonstrated by transient expression study and [^{3}H]GalCer loading study. Since the antibodies to epitope-tag are specific to the product of the transgene and do not cross-react with endogenous GALC, this method will particularly be useful in gene therapy experiments using normal cells or animals and the patient's cells that produce enzymatically defective but antigenic GALC protein.

Previous studies suggested that GALC protein is synthesized as 80–90 kDa precursor which is then cleaved to yield the 50 and 30 kDa subunits [19,20,31–33]. Consistently, cell extracts of transduced mouse fibroblasts in this study also showed bands at 80–90 and 30 kDa in Western blot analysis. However, the signal of the band near 30 kDa was very weak comparing with bands at 80–90 kDa. Two possible explanations of this finding are: (i) After the precursor being cleaved to 50 and 30 kDa subunits, the myc-epitope was removed from 30 kDa subunit either through proteolytic cleavage at the carboxyl terminus or non-specific degradation. (ii) Precursor form of human GALC protein could not be effectively cleaved to two subunits in the mouse fibroblasts because of species-specific or cell type-specific processing. Further experiments such as Western blot analysis of cell extracts using antibodies recognizing GALC protein or enzyme assay on lysosomal fraction from these cells is needed to clarify this question.

Transfection study in Bosc23 and NIH/3T3 cells showed that "original ATG" gave rise to similar or higher level of expression of GALC than "Kozak ATG"

or "1st ATG." While Chen et al. [19] have reported that modification of the sequences surrounding the initiation codon to more consensus one (A in position +4 to G) resulted in improved expression of GALC in COS-1 cells. This discrepancy suggested that although the sequence around the initiation codon in GALC gene is not optimal for translation according to Kozak rule, when GALC cDNA was driven by a strong heterologous promoter the expression level may be largely influenced by expression vectors and the host cell types rather than ATG surrounding sequence. In our earlier study [37], we reported higher GALC expression in "Kozak ATG" than "original ATG" as unpublished data, however by repeated experiments thereafter we found it should be revised.

Taken together, introduction of retrovirus into the SVZ of neonatal twitcher mouse resulted in stable transduction and expression of GALC in twitcher oligodendrocytes as analyzed by RT-PCR and immunohistochemistry and significant phenotypic improvements were achieved in these transduced oligodendrocytes. Obviously, the morphological aberrations and degeneration of twitcher oligodendrocytes in the CNS [7,8,40] or in culture systems [41,42] are caused by metabolic perturbation most likely the accumulation of psychosine, thus, morphological correction of transduced oligodendrocytes in this study probably reflects normalized biological functions of these cells. Further studies will be conducted to investigate whether and how these morphological corrections are related to functional improvements and myelin sheath preservation. We believe these basic studies will be useful for the development of future gene therapy approaches to treat this severe and fatal leukodystrophy.

Acknowledgments

We thank Kazuhiro Ikenaka (Department of Neural Information, National Institute for Physiological Sciences, Okazaki, Japan) and Tadanori Yoshimatsu (Institute for Biotechnology Research, Wakunaga Pharm., Hiroshima, Japan) for kindly providing the packaging cell line ψMP34 [24] and Masato Matsushima (Division of Clinical Research & Development, The Jikei University School of Medicine) for valuable advise on statistical analysis and Ryozo Gotoh (Laboratory Animal Center, The Jikei University School of Medicine) for technical assistance.

References

[1] D.A. Wenger, K. Suzuki, Y. Suzuki, K. Suzuki, Galactosylceramide lipidosis: globoid cell leukodystrophy (Krabbe disease), in: C.R. Scriver, A.L. Beaudet, W.S. Sly, D. Valle (Eds.), The Metabolic and Molecular Bases of Inherited Disease, McGraw-Hill, New York, 2001, pp. 3669–3694.

[2] T. Miyatake, K. Suzuki, Globoid cell leukodystrophy: additional deficiency of psychosine galactosidase, Biochem. Biophys. Res. Commun. 48 (1972) 538–543.

[3] K. Suzuki, Twenty-five years of the psychosine hypothesis: a personal perspective of its history and present status, Neurochem. Res. 23 (1998) 251–259.

[4] W. Krivit, E.G. Shapiro, C. Peters, J.E. Wagner, G. Cornu, J. Kurtzberg, D.A. Wenger, E.H. Kolodny, M.T. Vanier, D.J. Loes, K. Dusenbery, L.A. Lockman, Hematopoietic stem-cell transplantation in globoid-cell leukodystrophy, N. Engl. J. Med. 338 (1998) 1119–1126.

[5] K. Suzuki, K. Suzuki, The twitcher mouse: a model for Krabbe disease and for experimental therapies, Brain Pathol. 5 (1995) 249–258.

[6] N. Sakai, K. Inui, N. Tatsumi, H. Fukushima, T. Nishigaki, M. Taniike, J. Nishimoto, H. Tsukamoto, I. Yanagihara, K. Ozono, S. Okada, Molecular cloning and expression of cDNA for murine galactocerebrosidase and mutation analysis of the twitcher mouse, a model of Krabbe's disease, J. Neurochem. 66 (1996) 1118–1124.

[7] S.M. LeVine, M.V. Torres, Morphological features of degenerating oligodendrocytes in twitcher mice, Brain Res. 587 (1992) 348–352.

[8] M. Taniike, I. Mohri, N. Eguchi, D. Irikura, Y. Urade, S. Okada, K. Suzuki, An apoptotic depletion of oligodendrocytes in the twitcher, a murine model of globoid cell leukodystrophy, J. Neuropathol. Exp. Neurol. 58 (1999) 644–653.

[9] A.M. Yeager, S. Brennan, C. Tiffany, H.W. Moser, G.W. Santos, Prolonged survival and remyelination after hematopoietic cell transplantation in the twitcher mouse, Science 225 (1984) 1052–1054.

[10] P.M. Hoogerbrugge, K. Suzuki, K. Suzuki, B.J. Poorthuis, T. Kobayashi, G. Wagemaker, D.W. van Bekkum, Donor-derived cells in the central nervous system of twitcher mice after bone marrow transplantation, Science 239 (1988) 1035–1038.

[11] K. Suzuki, P.M. Hoogerbrugge, B.J. Poorthuis, D.W. Bekkum, K. Suzuki, The twitcher mouse. Central nervous system pathology after bone marrow transplantation, Lab. Invest. 58 (1988) 302–309.

[12] D.A. Wenger, E.Y. Snyder, R.M. Taylor, M.T. Vanier, M.A. Rafi, P. Luzi, J. Datto, Neural stem cells for the treatment of the twitcher mouse model of Krabbe disease, Am. J. Hum. Genet. 65 (1999) A116.

[13] J.S. Shen, K. Watabe, T. Ohashi, Y. Eto, Intraventricular administration of recombinant adenovirus to neonatal twitcher mouse leads to clinicopathological improvements, Gene Ther. 8 (2001) 1081–1087.

[14] C. Fantz, D.A. Wenger, M. Sands, Neonatal and in utero gene transfer utilizing adeno-associated virus and lentiviral vectors for the treatment of Krabbe's disease, Mol. Ther. 3 (2001) S228.

[15] Y.P. Wu, E.J. McMahon, J. Matsuda, K. Suzuki, G.K. Matsushima, K. Suzuki, Expression of immune-related molecules is down-regulated in twitcher mice following bone marrow transplantation, J. Neuropathol. Exp. Neurol. 60 (2001) 1062–1074.

[16] E. Costantino-Ceccarini, A. Luddi, M. Volterrani, M. Strazza, M.A. Rafi, D.A. Wenger, Transduction of cultured oligodendrocytes from normal and twitcher mice by a retroviral vector containing human galactocerebrosidase (GALC) cDNA, Neurochem. Res. 24 (1999) 287–293.

[17] A. Luddi, M. Volterrani, M. Strazza, A. Smorlesi, M.A. Rafi, J. Datto, D.A. Wenger, E. Costantino-Ceccarini, Retrovirus-mediated gene transfer and galactocerebrosidase uptake into twitcher glial cells results in appropriate localization and phenotype correction, Neurobiol. Dis. 8 (2001) 600–610.

[18] G.K. Matsushima, M. Taniike, L.H. Glimcher, M.J. Grusby, J.A. Frelinger, K. Suzuki, J.P. Ting, Absence of MHC class II molecules reduces CNS demyelination, microglial/macrophage infiltra-

tion, and twitching in murine globoid cell leukodystrophy, Cell 78 (1994) 645–656.
[19] Y.Q. Chen, M.A. Rafi, G. de Gala, D.A. Wenger, Cloning and expression of cDNA encoding human galactocerebrosidase, the enzyme deficient in globoid cell leukodystrophy, Hum. Mol. Genet. 2 (1993) 1841–1845.
[20] N. Sakai, K. Inui, N. Fujii, H. Fukushima, J. Nishimoto, I. Yanagihara, Y. Isegawa, A. Iwamatsu, S. Okada, Krabbe disease: isolation and characterization of a full-length cDNA for human galactocerebrosidase, Biochem. Biophys. Res. Commun. 198 (1994) 485–491.
[21] M. Kozak, The scanning model for translation: an update, J. Cell Biol. 108 (1989) 229–241.
[22] N. Sakai, H. Fukushima, K. Inui, L. Fu, T. Nishigaki, I. Yanagihara, N. Tatsumi, K. Ozono, S. Okada, Human galactocerebrosidase gene: promoter analysis of the 5′-flanking region and structural organization, Biochim. Biophys. Acta 1395 (1998) 62–67.
[23] J.S. Shen, X.L. Meng, T. Yokoo, K. Sakurai, K. Watabe, T. Ohashi, Y. Eto, Widespread and highly persistent gene transfer to the CNS by retrovirus vector in utero: implication for gene therapy to Krabbe disease, J. Gene Med. (in press).
[24] T. Yoshimatsu, M. Tamura, S. Kuriyama, K. Ikenaka, Improvement of retroviral packaging cell lines by introducing the polyomavirus early region, Hum. Gene Ther. 9 (1998) 161–172.
[25] N.E. Bowles, R.C. Eisensmith, R. Mohuiddin, M. Pyron, S.L. Woo, A simple and efficient method for the concentration and purification of recombinant retrovirus for increased hepatocyte transduction in vivo, Hum. Gene Ther. 7 (1996) 1735–1742.
[26] S.W. Levison, J.E. Goldman, Both oligodendrocytes and astrocytes develop from progenitors in the subventricular zone of postnatal rat forebrain, Neuron 10 (1993) 201–212.
[27] S. Raghavan, A. Krusell, Optimal assay conditions for enzymatic characterization of homozygous and heterozygous twitcher mouse, Biochim. Biophys. Acta 877 (1986) 1–8.
[28] T. Kobayashi, N. Shinnoh, Y. Kuroiwa, Metabolism of galactosylceramide in the twitcher mouse, an animal model of human globoid cell leukodystrophy, Biochim. Biophys. Acta 879 (1986) 215–220.
[29] T. Kobayashi, N. Shinnoh, Y. Kuroiwa, Metabolism of ceramide trihexoside in cultured skin fibroblasts from Fabry's patients, carriers and normal controls, J. Neurol. Sci. 65 (1984) 169–177.
[30] L.W. Swanson, Brain Maps: Structure of the Rat Brain, Elsevier Science, Amsterdam, 1998.
[31] Y.Q. Chen, D.A. Wenger, Galactocerebrosidase from human urine: purification and partial characterization, Biochim. Biophys. Acta 1170 (1993) 53–61.
[32] N. Sakai, K. Inui, M. Midorikawa, Y. Okuno, S. Ueda, A. Iwamatsu, S. Okada, Purification and characterization of galactocerebrosidase from human lymphocytes, J. Biochem. (Tokyo) 116 (1994) 615–620.
[33] S. Nagano, T. Yamada, N. Shinnoh, H. Furuya, T. Taniwaki, J. Kira, Expression and processing of recombinant human galactosylceramidase, Clin. Chim. Acta 276 (1998) 53–61.
[34] S. Szuchet, The morphology and ultrastructure of oligodendrocytes and their functional implications, in: H. Kettenmann, B.R. Ransom (Eds.), Neuroglia, Oxford University Press, New York, 1995, pp. 23–43.
[35] F.A. Tansey, W. Cammer, A pi form of glutathione-*S*-transferase is a myelin- and oligodendrocyte-associated enzyme in mouse brain, J. Neurochem. 57 (1991) 95–102.
[36] M.A. Rafi, J. Fugaro, S. Amini, P. Luzi, G. de Gala, T. Victoria, C. Dubell, M. Shahinfar, D.A. Wenger, Retroviral vector-mediated transfer of the galactocerebrosidase (GALC) cDNA leads to overexpression and transfer of GALC activity to neighboring cells, Biochem. Mol. Med. 58 (1996) 142–150.
[37] J.S. Shen, K. Watabe, X.L. Meng, H. Ida, T. Ohashi, Y. Eto, Establishment and characterization of spontaneously immortalized Schwann cells from murine model of globoid cell leukodystrophy (twitcher), J. Neurosci. Res. 68 (2002) 588–594.
[38] S.P. Forestell, E. Bohnlein, R.J. Rigg, Retroviral end-point titer is not predictive of gene transfer efficiency: implications for vector production, Gene Ther. 2 (1995) 723–730.
[39] R. De Gasperi, V.L. Friedrich, G.M. Perez, E. Senturk, P.H. Wen, K. Kelley, G.A. Elder, M.A. Gama Sosa, Transgenic rescue of Krabbe disease in the twitcher mouse, Gene Ther. 11 (2004) 1188–1194.
[40] H. Takahashi, H. Igisu, K. Suzuki, K. Suzuki, The twitcher mouse: an ultrastructural study on the oligodendroglia, Acta Neuropathol. (Berl) 59 (1983) 159–166.
[41] H. Nagara, H. Ogawa, Y. Sato, T. Kobayashi, K. Suzuki, The twitcher mouse: degeneration of oligodendrocytes in vitro, Brain Res. 391 (1986) 79–84.
[42] H. Ida, F. Kawame, S.U. Kim, Y. Eto, Abnormality in cultured oligodendrocytes and Schwann cells isolated from the twitcher mouse, Mol. Chem. Neuropathol. 13 (1990) 195–204.

European Journal of Neuroscience, Vol. 19, pp. 55–64, 2004

Synthesis, localization and externalization of galectin-1 in mature dorsal root ganglion neurons and Schwann cells

Kazunori Sango,[1] Akiko Tokashiki,[1] Kyoko Ajiki,[1] Masao Horie,[1] Hitoshi Kawano,[1] Kazuhiko Watabe,[2] Hidenori Horie[3,4] and Toshihiko Kadoya[5]

[1]Department of Developmental Morphology, Tokyo Metropolitan Institute for Neuroscience, 2–6 Musashidai, Fuchu-shi, Tokyo 183–8526, Japan

[2]Department of Molecular Neuropathology, Tokyo Metropolitan Institute for Neuroscience, Fuchu-shi, Tokyo 183–8526, Japan

[3]Advanced Research Center for Biological Science, Waseda University, 2-7-5 Higashifushimi, Nishitokyo-shi, Tokyo 202–0021, Japan

[4]Brain Information Science Institute, Corporate Research Center, Fuji Xerox, 430 Sakai, Nakai-machi, Ashigarakami-gun, Kanagawa 259–0157, Japan

[5]R&D Center, Production Department, Pharmaceutical Division, Kirin Brewery Co. Ltd, Takasaki, Gunma 370–0013, Japan

Keywords: adult rat, β-galactoside binding lectin, extracellular release, mouse cell line, peripheral nerve

Abstract

We recently confirmed that oxidized galectin-1 is a novel factor enhancing axonal growth in peripheral nerves after axotomy, but the process of extracellular release and oxidization of endogenous galectin-1 in the injured nervous tissue remains unknown. In the present study, we examined the distribution of galectin-1 in adult rat dorsal root ganglia (DRG) *in vivo* and *in vitro*. By RT-PCR analysis and *in situ* hybridization histochemistry, galectin-1 mRNA was detected in both DRG neurons and non-neuronal cells. Immunohistochemical analyses revealed that galectin-1 was distributed diffusely throughout the cytoplasm in smaller diameter neurons and Schwann cells in DRG sections. In contrast, the immunoreactivity for galectin-1 was detected in almost all DRG neurons from an early stage in culture (3 h after seeding) and was restricted to the surface and/or extracellular region of neurons and Schwann cells at later stages in culture. In a manner similar to the primary cultured cells, we also observed the surface and extracellular expression of this molecule in immortalized adult mouse Schwann cells (IMS32). Western blot analysis has revealed that both reduced and oxidized forms of galectin-1 were detected in culture media of DRG neurons and IMS32. These findings suggest that galectin-1 is externalized from DRG neurons and Schwann cells upon axonal injury. Some of the molecules in the extracellular milieu may be converted to the oxidized form, which lacks lectin activity but could act on neural tissue as a cytokine.

Introduction

Galectin-1 is a member of the galectins, a family of β-galactoside-binding animal lectin (Barondes *et al.*, 1994; Cooper & Barondes, 1999). It is a homodimer with a subunit molecular weight of 14.5 kDa and exhibits lectin activity only in the reduced form (de Waard *et al.*, 1976; Kasai & Hirabayashi, 1996; Perillo *et al.*, 1998). It has been suggested that this lectin plays roles in a wide variety of biological functions such as cell growth and differentiation, apoptosis, cell adhesion, tumour spreading, neurite outgrowth and inflammatory response (Outenreath & Jones, 1992; Mahanthappa *et al.*, 1994; Perillo *et al.*, 1995, 1998; Puche *et al.*, 1996; Rabinovich *et al.*, 2000a,b, 2002). Despite lacking a signal leading peptide, galectin-1 has been reported as being externalized from myogenic cells (Cooper & Barondes, 1990), neuroblastoma cells (Avellana-Adalid *et al.*, 1994), Chinese hamster ovary (CHO) cells (Cho & Cummings, 1995) and human leukaemia cell lines (Lutomski *et al.*, 1997). These findings suggested a pathway for the extracellular release of galectin-1 which is distinct from the classic secretory pathway (Cooper & Barondes, 1990; Cleves *et al.*, 1996; Hughes, 1999). Some other members of galectin family, namely galectin-3 (Mehul & Hughes, 1997) and galectin-4 (Danielsen & van Deurs, 1997), are subject to externalization in a manner similar to galectin-1. It has been suggested that, following externalization, some of the galectin molecules associate with surface or extracellular matrix glycoconjugates where lectin activity is stabilized while the others, free from glycoconjugate ligands, are rapidly oxidized and inactivated in the nonreducing extracellular environment (Tracey *et al.*, 1992; Cho & Cummings, 1995). In contrast to the concept that galectin-1 is biologically active only in the reduced form, we introduced oxidized galectin-1 as a novel factor enhancing axonal regeneration in peripheral nerves (Horie *et al.*, 1999; Inagaki *et al.*, 2000; Fukaya *et al.*, 2003). Oxidized galectin-1 lacked lectin activity, but it exhibited marked axonal regeneration-promoting activity at concentrations (pg/mL range) substantially lower than those at which the lectin effects of galectin-1 were exhibited in neuronal cells *in vitro* (> ng/mL) (Outenreath & Jones, 1992; Puche *et al.*, 1996). Taking these findings into consideration, oxidized galectin-1 is likely to act on nervous tissue not as a lectin but as a cytokine.

Galectin-1 is expressed in dorsal root ganglion (DRG) neurons and motor neurons with immunoreactivity localized to neuronal cell bodies, axons and Schwann cells of adult rodents (Regan *et al.*, 1986; Hynes *et al.*, 1990; Fukaya *et al.*, 2003). After axonal injury, cytosolic reduced galectin-1 is likely to be externalized from growing

Correspondence: Dr Kazunori Sango, as above.
E-mail: kazsango@tmin.ac.jp

Received 4 June 2003, revised 27 September 2003, accepted 22 October 2003

doi:10.1046/j.1460-9568.2003.03102.x

axons and reactive Schwann cells to an extracellular space, where some of the molecule may be converted to the oxidized form and enhance axonal regeneration (Horie & Kadoya, 2000). However, extracellular release of galectin-1 from mature neurons and/or non-neuronal cells after axotomy remains to be clarified. In the present study, we examined histochemical localization of galectin-1 in adult rat DRG both *in vivo* and *in vitro*.

Materials and methods

Animals

Three-month-old female Sprague-Dawley rats were used. All experiments were conducted in accordance with the Guideline for the Care and Use of Animals (Tokyo Metropolitan Institute for Neuroscience, 2000).

RT-PCR analysis

The rats were anaesthetized with ether and killed. Thirty-five DRG (from the cervical to sacral levels) with associated nerve bundles and kidneys were dissected and removed from each animal. Nerve bundles were severed from ganglia, using a sharp blade. Each tissue (ganglia, spinal nerve fibres or kidneys) was separately collected in a sterile tube and stored at −80 °C. Total RNA was isolated from these tissues using Trizol reagent (Invitrogen, Groningen, Netherlands), and was reverse transcribed with M-MLV reverse transcriptase (Invitrogen) and $pd(N)_6$ random primer (Amersham Biosciences Corp., Piscataway, NJ, USA) (Sango *et al.*, 2002b). The synthesized cDNA was used as a template for the PCR reaction. The PCR primers were designed to amplify the 408 bp of rat galectin-1 open reading frame; sense primer, 5′-ATGGCCTGTGGTCTGGTCGCC-3′ and antisense primer, 5′-TCAC-TCAAAGGCCACACACTT-3′ (GenBank Accession No. M19036) (Clerch *et al.*, 1988). PCR was performed in a 25-μL mixture solution containing 0.2 mM dNTP mix, 10× PCR buffer with 25 mM $MgCl_2$, 0.5 μM of each primer and 0.625 U of AmpliTaq Gold DNA polymerase (Applied Biosystems, Foster City, CA, USA). After denaturation at 95 °C for 9 min, the PCR reaction was cycled 30 times at 95 °C for 1 min, 55 °C for 1 min and 72 °C for 2 min. The PCR products were separated by electrophoresis through 2% agarose gel and visualized with ethidium bromide staining.

Preparation of the plasmid containing rat galectin-1 cDNA

The plasmid containing the rat galectin-1 cDNA fragment was created by PCR cloning as described previously (Toba *et al.*, 2002). Briefly, the 408-bp fragment amplified by PCR was subcloned into pGEM-T Easy Vector (Promega Corp., Madison, WI, USA) according to the manufacturer's instructions, and the resulting plasmid DNA was sequenced (Sawady Custom Technology Service, Tokyo, Japan).

In situ *hybridization*

We examined mRNA expression patterns of galectin-1 by *in situ* hybridization histochemistry as described previously (Ichikawa *et al.*, 1997) with slight modifications. Digoxigenin-labelled antisense and sense cRNA probes for galectin-1 were prepared using DIG RNA labelling mix (Roche Diagnostics, GmbH, Mannheim, Germany) with linearized plasmid DNA according to the manufacturer's instructions. The rats were anaesthetized by intraperitoneal injection of pentobarbital sodium (50 mg/kg), and then briefly perfused through the left cardiac ventricle with 100 mM phosphate-buffered saline (PBS, pH 7.4) followed by 4% paraformaldehyde. Lumbar DRG dissected from the rats were processed for paraffin embedding and sectioned into 5-μm-thick slices. Deparaffinized sections were treated with 0.2 N HCl for 15 min, 0.2% triton-X for 10 min at room temperature, and proteinase-K (Invitrogen, 2 mg/mL in 100 mM PBS) for 20 min at 37 °C, postfixed with 4% paraformaldehyde in 100 mM PBS for 10 min, and treated with 2 mg/mL glycine in 100 mM PBS for 20 min at room temperature. The hybridization buffer contained 50% formamide, 300 mM NaCl, 2.5 mM EDTA, 0.5 mg/mL Escherichia coli tRNA, 20 mM Tris–HCl (pH 8.0), 1 × Denhardt's solution (Eppendorf, Hamburg, Germany). Both the antisense and the sense probes were diluted to a final concentration of 310 ng/mL. Hybridizations were performed overnight at 50 °C. Thereafter, the samples were washed in 2 × standard saline citrate (SSC; 1 × SSC = 150 mM NaCl, 15 mM sodium citrate) containing 50% formamide for 1 h at 50 °C, followed by 2 × 5 min in 10 mM Tris–HCl (pH 8.0) containing 500 mM NaCl at room temperature, 30 min in 10 mM Tris–HCl (pH 8.0) containing 20 μg/mL RNase A and 500 mM NaCl at 37 °C, 2 × 5 min in 10 mM Tris–HCl (pH 8.0) containing 500 mM NaCl at room temperature, 2 × 30 min in 1 × SSC containing 50% formamide at 50 °C, and finally 3 × 5 min in 100 mM Tris–HCl (pH 7.5) containing 150 mM NaCl at room temperature. The digoxigenin-labelled probes were detected using alkaline-phosphatase-conjugated antidigoxigenin (Roche Diagnostics). The positive signal was detected as a dar' precipitate (BCIP/NBT; 5-bromo-4-chloro-3-indoyl-phosphate p-toluidine salt/4-nitroblue tetrazolium chloride). Tissue sections were then mounted with Crystal/Mount (Biomeda Corp., Foster City, CA, USA) without cover glasses and dried at 70 °C.

Immunohistochemistry

The rats were anaesthetized using pentobarbital sodium as described above and perfused through the left cardiac ventricle with 100 mM PBS followed by acid–alcohol (95% ethanol and 5% acetic acid). DRG dissected from the rats were processed for paraffin embedding and sectioned into 5-μm-thick slices. Deparaffinized sections were incubated overnight at 4 °C with rabbit antigalectin-1 polyclonal antibody (1 : 1000, diluted with 0.5% skimmed milk) (Horie *et al.*, 1999). After rinsing with distilled water, the sections were incubated for 1 h at 37 °C with peroxidase-conjugated antirabbit IgG antibody (1 : 100; Vector Laboratories Inc., Burlingame, CA, USA). The immunoreaction was visualized under a light microscope using 0.01% diaminobenzidine tetrahydro-chloride (DAB; Wako Co., Tokyo, Japan) and 0.01% hydrogen peroxide in 50 mM Tris buffer (pH 7.4) at 37 °C for 15 min (Kawano *et al.*, 1999).

Cultures

The rats were killed by ether exposure. Primary culture of adult DRG neurons was performed as previously described (Sango *et al.*, 1991). Briefly, 20–25 ganglia (from the thoracolumbar level) were dissected from each animal and dissociated with collagenase (Worthington Biochem., Freehold, NJ, USA) and trypsin (Sigma, St Louis, MO, USA). These ganglia were subjected to density gradient centrifugation (5 min, 200 *g*) with 30% Percoll (Pharmacia Biotech, Uppsala, Sweden) to eliminate the myelin sheath. This procedure resulted in a yield of $>5 \times 10^4$ neurons together with a smaller number of non-neuronal cells such as Schwann cells, satellite cells and fibroblasts. The cells were suspended in Ham's F12 (Invitrogen) containing 10% fetal calf serum (Mitsubishi Kasei Co. Ltd, Tokyo, Japan), and seeded on poly L-lysine (PL, Sigma, 10 μg/mL)-coated wells of 8-well chamber slides (Nalge Nunc International, Naperville, IL, USA) or PL-coated Aclar fluorocarbon coverslips (Nissin EM Co. Ltd, Tokyo, Japan; 9 mm in diameter) in 60-mm culture dishes (Falcon, Lincoln Park, NJ, USA). The density of neurons was adjusted to $\approx 2 \times 10^3/cm^2$ in each well or coverslip. After remaining in serum-containing medium for 12 h, cells were cultured in serum-free medium [Ham's F12 with B27 supplement (Invitrogen)] for up to 7 days.

A spontaneously immortalized Schwann cell line established from adult ICR mice, IMS32 (Watabe *et al.*, 1995) were seeded on culture flasks (Nalge Nunc) at a density of $5 \times 10^4/cm^2$ and maintained in Dulbecco's Modified Eagles medium (DMEM; Sigma) supplemented with 5% FCS. When the cell density reached confluence, cells were trypsinized and reseeded on coverslips at a density of $1–2 \times 10^4/cm^2$ or collected to extract total RNA for use in Northern blotting. Cells seeded on coverslips were kept in DMEM with B27 supplement for up to 7 days.

Immunocytochemistry

Cells dissociated from DRG after 3 or 12 h or 2, 4 or 7 days in culture and IMS32 cells after 1, 2 or 4 days of seeding on coverslips were fixed with acid–alcohol for 30 min at room temperature. The fixed cells were incubated overnight at 4 °C with rabbit antigalectin-1 polyclonal antibody (1 : 3000). After rinsing with PBS, the cells were incubated for 1 h at 37 °C with peroxidase-conjugated antirabbit IgG antibody (1 : 100, Vector Laboratories). The immunoreaction was visualized as described above.

Double immunofluorescent staining

To verify that both neurons and Schwann cells are immunoreactive for galectin-1, double immunostaining for neurofilament and galectin-1, or S100 protein and galectin-1 in cultured DRG cells was performed. Two different fixatives were used, depending on the antigen to be examined: acid–alcohol for detection of neurofilament and alcoholic formaldehyde (85% ethanol, 4% formaldehyde and 5% acetic acid) for detection of S100. Fixed cells were incubated overnight at 4 °C with a mixture of rabbit antigalectin-1 polyclonal antibody (1 : 1000) and mouse antineurofilament 200 monoclonal antibody (1 : 1000; Sigma) or mouse anti-S100 monoclonal antibody (1 : 100, Chemicon International, Inc., Temecula, CA, USA). After rinsing with PBS, they were then incubated in a mixture of fluorescein isothiocyanate (FITC)-conjugated antirabbit IgG (1 : 100, Vector Laboratories) and biotinylated antimouse IgG (1 : 100) for 1 h at 37 °C. Finally, cells were incubated with streptavidin–Texas Red (1 : 100, Vector Laboratories) for 1 h at room temperature.

Image presentation

Sections processed for *in situ* hybridization and immunohistochemistry and cell culture samples processed for immunocytochemistry were observed and recorded using a Zeiss Axiophoto microscope (Carl Zeiss Co. Ltd, Germany) equipped with a cooled CCD camera (Zeiss AxioCam) and Zeiss Axiovision software. The digital images were manually aligned using PhotoShop 4.0 (Adobe Systems Incorporated, Mountain View, CA, USA) to equalize tone and contrast.

Immunoelectron microscopy

Cells dissociated from DRG and IMS32 cells on coverslips were kept in the serum-free medium for 7 days and fixed with 4% paraformaldehyde, 0.05% glutaraldehyde and 0.2% picric acid for 30 min at room temperature (Llewellyn-Smith *et al.*, 1985). The fixed cells were incubated overnight at 4 °C with rabbit antigalectin-1 polyclonal antibody (1 : 1000). After rinsing with PBS, the cells were incubated for 1 h at 37 °C with 1.4 nm Nanogold-conjugated antirabbit IgG antibody (1 : 100; Nanoprobes, Yaphank, NY, USA). After the postfix with 1% glutaraldehyde and silver enhancement according to the manufacturer's instruction, the samples were processed for embedding in epoxy resin for observation using an electron microscope (Sango *et al.*, 2002a).

Northern blot analysis

The galectin-1 cDNA fragment (10 ng/μL) was prepared from the plasmid, and labelled with alkaline phosphatase (AlkPhos Direct; Amersham Biosciences) according to the manufacturer's instructions. Northern blotting was performed on total RNA isolated from confluent cultures of IMS32 in a culture flask. Twenty micrograms of RNA was electrophoresed in 1% agarose–formaldehyde gel, transferred to Hybond N+ membrane (Amersham Biosciences) and hybridized overnight at 55 °C with the labelled probe. The CDP-Star™ chemiluminescent detection reagent (Amersham Biosciences) was used for visualization of the positive signals (Zajc Kreft *et al.*, 2000).

Western blot analysis

DRG neurons seeded at a high density ($> 5 \times 10^3/cm^2$) in each well of an 8-well chamber slide and confluent cultures of IMS32 cells in a flask were washed three times with serum-free medium (F12 supplemented with B27) and incubated for 48 h in serum-free medium. The conditioned medium from each of the cells was centrifuged (5 min, 200 *g*) and subjected to SDS–polyacrylamide gel electrophoresis (SDS-PAGE). SDS-PAGE was performed under reducing–nonreducing conditions using 15–25% polyacrylamide gradient gel. After electrophoresis, the proteins were transferred onto a polyvinylidene difluoride (PVDF) membrane with semidry electroblotter (Owl Scientific Inc., Woburn, MA, USA). The membrane was incubated with antigalectin-1 polyclonal antibody (1 μg/mL) for 1 h after blocking with Block Ace (Snow Brand, Tokyo, Japan). After rinsing with Tris-buffered saline (TBS), the membrane was incubated in a solution of biotinylated antirabbit IgG (1 : 3000, DAKO, Carpinteria, CA, USA) for 1 h. Then, after rinsing, the membrane was incubated with HRP-conjugated streptavidin (1 : 3000, DAKO) for 1 h. Immunocomplexes on the membrane were visualized by chemiluminesence using the Super-Signal West Femto Maximum Sensitivity Substrate (Pierce Biotechnology Inc., Rockford, IL, USA) and LAS 1000 Image Analyser (Fuji Film, Tokyo, Japan).

Results

Galectin-1 mRNA expression in adult rat DRG

RT-PCR analysis showed mRNA expressions of galectin-1 in all tissues examined, i.e. dorsal root ganglia (containing both neurons and non-neuronal cells), spinal nerve fibres (neuronal cell bodies were excluded) and kidneys as a positive control (Fig. 1). This result implies that both neurons and non-neuronal cells synthesize the lectin molecule. By using *in situ* hybridization histochemistry with digoxigenin-labelled cRNA probe, galectin-1 mRNA was abundantly detected in all neurons in the sections of adult rat DRG (Fig. 2). In general, the staining intensity in smaller diameter neurons was higher than that in larger diameter neurons. These findings are in agreement with those of a previous study (Hynes *et al.*, 1990), in which a ^{35}S-labelled cRNA probe was used for *in situ* hybridization. The mRNA expression in non-neuronal cells (Schwann cells, satellite cells etc.) was much weaker than that in neurons. The positive reactions would seem to be specific for galectin-1 mRNA because the sense probe of galectin-1 failed to hybridize in the tissue (Fig. 2).

Immunohistochemical localization of galectin-1 in DRG in vivo *and* in vitro

Intense immunoreactivity for galectin-1 was detected in a subset of neurons (arrows in Fig. 3A) and Schwann cells (arrowheads in Fig. 3A) in the sections of adult rat DRG. We counted the number of immunoreactive and nonimmunoreactive neurons in three sections of

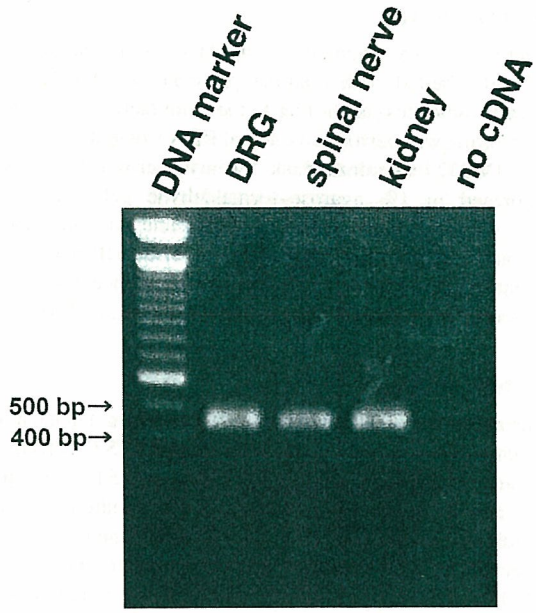

FIG. 1. Galectin-1 mRNA expression in DRG and peripheral nerves: RT-PCR analysis. The photograph of gel electrophoresis (from the left to the right lanes) indicates a DNA marker (100-bp DNA ladder; Invitrogen), PCR products from cDNA of adult rat DRG, spinal nerves and kidneys (as a positive control), and a PCR reaction without a template cDNA (as a negative control), respectively.

different ganglia in each rat. The ratio of galectin-1-immunoreactive neurons was 26.1 ± 1.9% (mean ± SEM from nine sections, 1582 neurons from three animals). Most of the immunoreactive neurons were small or intermediate (< 30 μm) in diameter, which was consistent with previous findings (Regan *et al.*, 1986). This positive reaction was completely eliminated by preabsorption of antigalectin-1 with antigen (not shown), suggesting its specificity for galectin-1. In contrast to the *in vivo* results, galectin-1 immunoreactivity was detected in almost all neurons at all culture times (Fig. 3B–E). The immunoreactivity had spread throughout the cytoplasm by 3 h (Fig. 3B) in culture, but was localized to the surface of neurons after 2 days in culture (Fig. 3C and D). Double immunofluorescent staining with antineurofilament antibody (Fig. 4A–C) showed localization of galectin-1 to neuronal cell bodies but not to neurites, when neurons were cultured in serum-free medium. In contrast, the intense immunoreactivity for galectin-1 was detected in both neuronal cell bodies and neurites in culture in the presence of serum (Fig. 4D–F). At early stages (3 h, 12 h and 2 days) of culture, most galectin-1-immunoreactive cells were neurons. In contrast, the immunoreactivity for galectin-1 was detected in both neurons and non-neuronal cells, especially spindle-shaped cells (arrows in Fig. 3E), at later stages (4 and 7 days) of culture. The spindle-shaped cells were immunoreactive for S100 (Fig. 4G–I) and were identified as Schwann cells. At a higher magnification, the immunoreactivity for galectin-1 was scattered throughout Schwann cells and localized at the cell surface (Fig. 3F).

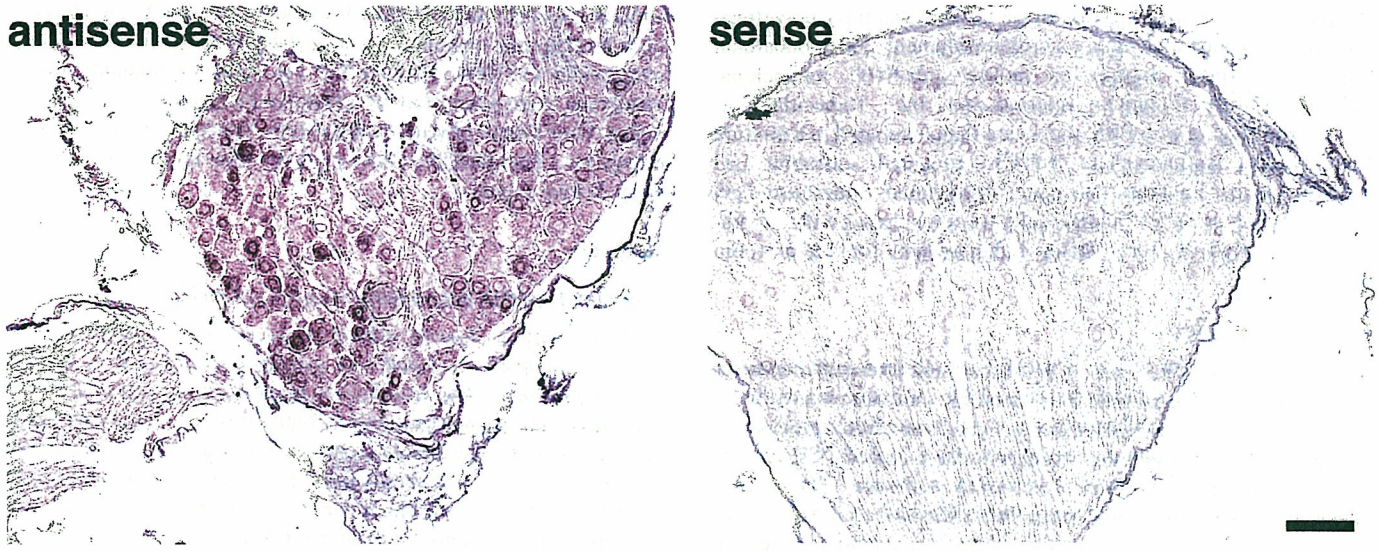

FIG. 2. *In situ* hybridization histochemistry complementary to galectin-1 mRNA in the adult rat DRG. Hybridization with an antisense probe (left panel) revealed galectin-1 mRNA expression in all neurons, with a tendency for more intense signals to be observed in smaller neurons than in larger ones. Hybridization with a sense probe (right panel) resulted in no signals. Scale bar, 100 μm.

FIG. 3. Immunohistochemical localization of galectin-1 in adult rat DRG (A) *in vivo* and (B–F) *in vitro*. (A) Galectin-1 immunoreactivity was observed diffusely in the cytosol of small neurons (arrows) and Schwann cells (arrowheads). The section was counterstained with haematoxylin. (B–F) The immunostaining was carried out after (B) 3 h, (C) 2, (D) 4 and (E and F) 7 days in culture. Galectin-1 immunoreactivity was throughout the cytosol of almost all neurons after 3 h in culture (B), but became concentrated at the cell surface beyond 2 days in culture (C–E). After 7 days in culture (E), not only neurons but also Schwann cells (arrows) were immunoreactive for galectin-1. At a higher magnification (F), galectin-1 immunoreactivity was scattered throughout Schwann cells and localized at the cell surface. Scale bars, 50 μm (A), 50 μm (in E for B to E), 25 μm (F).

FIG. 4. Immunofluorescence micrographs of adult rat DRG neurons (A–F) and Schwann cells (G–I) after 7 days in culture, stained with antibodies to galectin-1 (green; A, D and G) and neurofilament (red; B and E) or S100 (red; H). A and B are merged into C, D and E are merged into F, and G and H are merged into I. (A–C) When neurons were cultured in serum-free medium, galectin-1 is localized to the cytoplasm near the surface of the neuronal cell bodies, but not to the neurites. (D–F) When neurons were cultured in serum-containing medium, the immunoreactivity for galectin-1 was detected in both neuronal cell bodies and neurites. (G–I) Galectin-1 immunoreactivity is observed in both the cytoplasm of Schwann cells and extracellular regions. Scale bars, 50 μm (A–F), 30 μm (G–I).

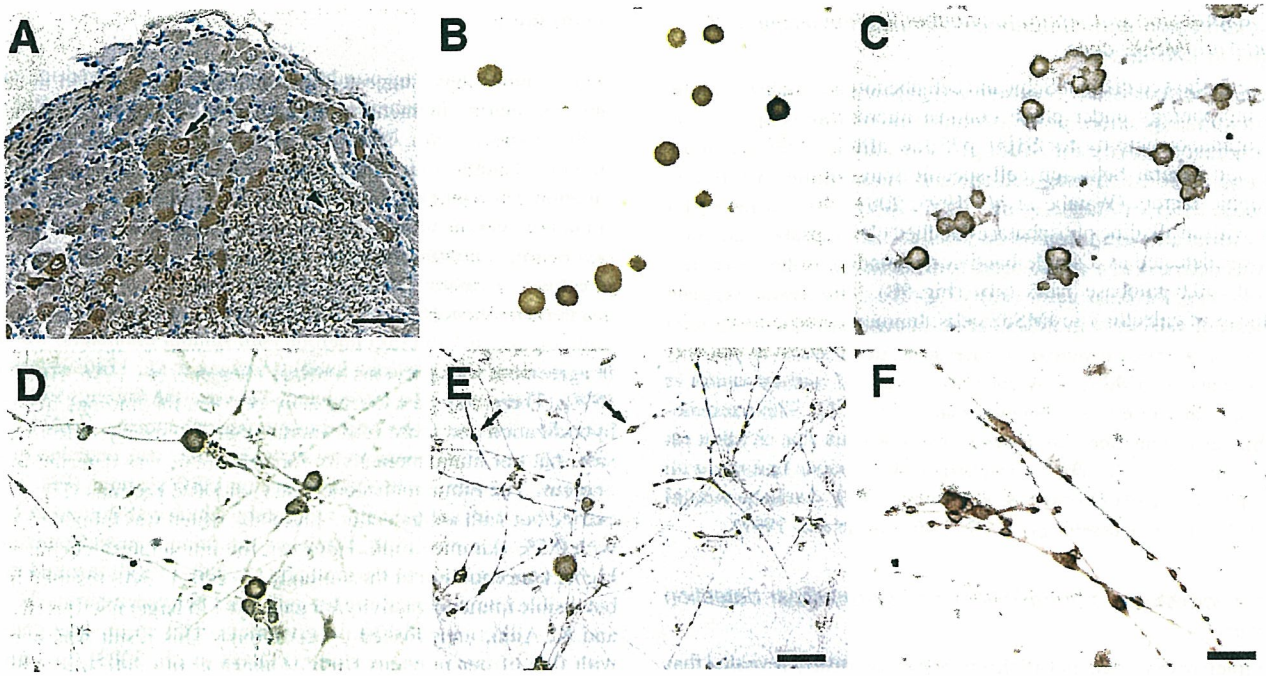

FIG. 3.

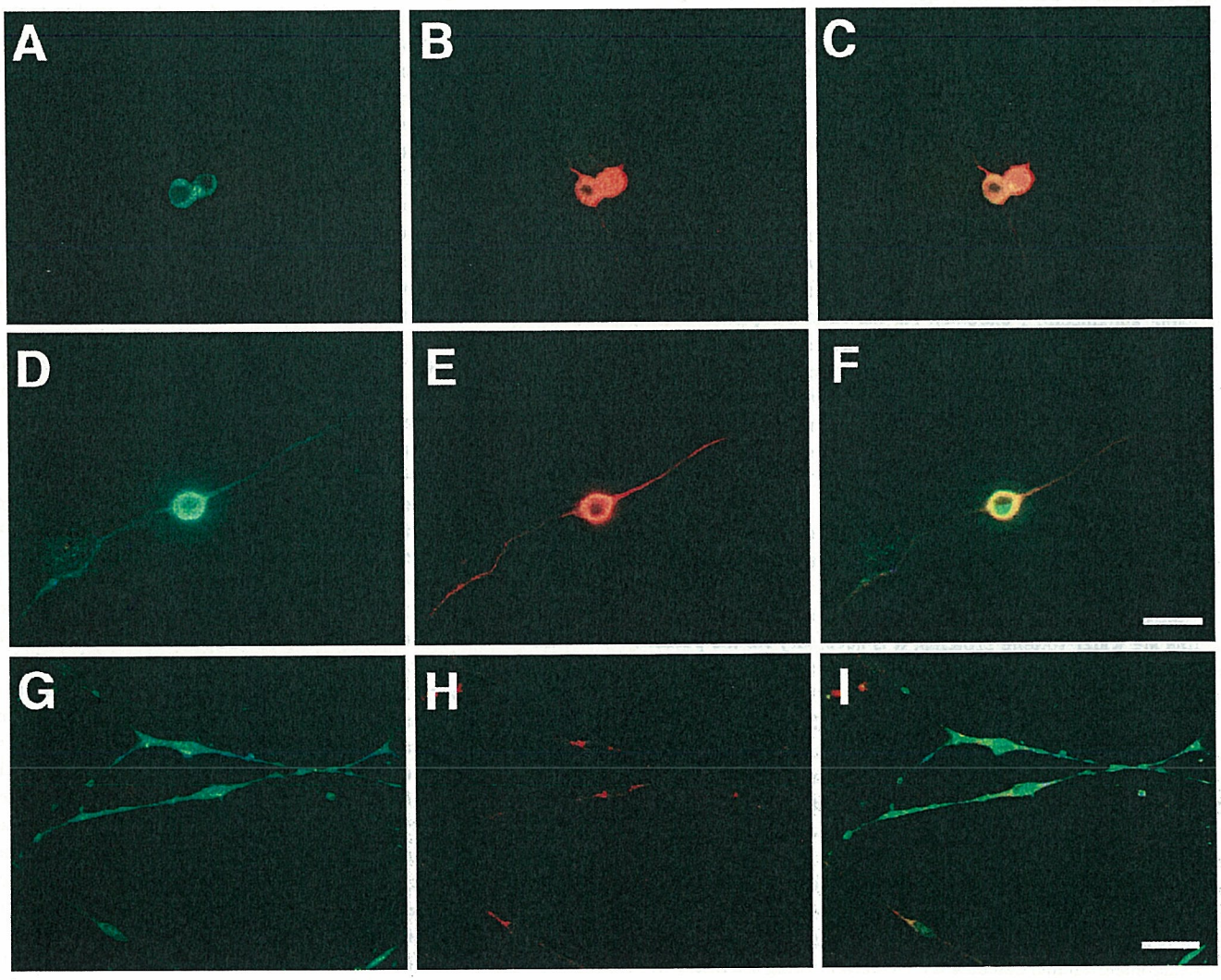

FIG. 4.

mRNA expression and immunocytochemical localization of galectin-1 in IMS32 cells

IMS32 cells showed distinct Schwann cell phenotypes, such as spindle shaped morphology under phase contrast microscopy (Fig. 5A) and intense immunoreactivity for S100, p75 low affinity NGF receptors, laminin and several Schwann cell-specific transcription factors and neurotrophic factors (Watabe *et al.*, 1995, 2003). By Northern blot analysis with an alkaline phosphatase-labelled cDNA probe, galectin-1 mRNA was detected as a single band corresponding to the molecular weight of ≈0.6 kilobase pairs (kb) (Fig. 5B). This result suggests biosynthesis of galectin-1 in IMS32 cells. Immunocytochemistry with antigalectin-1 antibody revealed the intense immunoreactivity not only in the cytoplasm of IMS32 cells but also on the cell surface and/or in the extracellular space with vesicular shapes (Fig. 5C). This immunohistochemical appearance was more prominent than that in adult rat Schwann cells (Fig. 3F), and is consistent with previous findings with different kinds of cells (Cooper & Barondes, 1990; Avellana-Adalid *et al.*, 1994; Cho & Cummings, 1995; Lutomski *et al.*, 1997).

Electron microscopy for intracellular and extracellular detection of galectin-1

Electron microscopic studies with immunocytochemistry revealed that the immnogold labelling was found mainly at the periphery and/or outside the soma of DRG cells (Fig. 6A) and IMS32 cells (Fig. 6B). Substitution of the primary antibody with preimmune rabbit IgG resulted in no staining (Fig. 6C). The intracellular electron-dense materials (indicated as asterisks in Fig. 6A and C) appear to be lysosomes.

Detection of galectin-1 in the culture medium of DRG neurons and IMS32 cells

The findings from immunocytochemistry (Figs 3–6) suggested that galectin-1 was externalized from DRG cells (neurons and Schwann cells) and IMS32 cells to culture media. To confirm this, we collected the conditioned media from these cells and analysed them by Western blots using antigalectin-1 antibody. As shown in our previous study (Inagaki *et al.*, 2000), the average molecular mass of recombinant human galectin-1 purified from COS1 cells (oxidized form, Fig. 7, lane 4) was slightly smaller than that of the reduced form of the protein (Fig. 7, lane 1). Under the condition without a reducing agent, both reduced and oxidized forms of galectin-1 were detected in culture medium of IMS32 (Fig. 7, upper panel, lane 3) and DRG neurons (Fig. 7, lower panel, lane 3).

Very few trypan-blue-positive IMS32 cells were observed (< 0.1% of the cells at any observation area) at 48 h after seeding (not shown), suggesting that cell death was so low that it could not have contributed to galectin-1 in the conditioned medium. Although galectins are water-soluble proteins, it is necessary for the purification of cytosolic galectins to add some hapten sugars such as lactose to an extraction buffer (Kasai & Hirabayashi, 1996). This means that the lectin molecules can hardly be dissociated from water-insoluble substances of cells without the hapten sugars, when cells are damaged or lysed. The serum-free culture medium used for the release experiments in this study did not contain lactose or other galactose-containing saccharides. Supposing cell death and lysis occurred during the culture in the medium, it would be hardly possible for galectin-1 or other galectins to be separated from water-insoluble materials of dead cells and move from the cytosol to the culture supernatants. Therefore, most galectin-1 molecules in the culture supernatants detected by Western blotting are likely to be those which were externalized from viable cells.

Discussion

Many studies have suggested that galectins are involved in cell–cell and cell–matrix interactions during neural development (Puche *et al.*, 1996; Pesheva *et al.*, 1998) and progression and migration of brain tumours (Camby *et al.*, 2001; Lahm *et al.*, 2001). However, much less attention has been paid to the functional significance of the molecules in mature nervous tissues. In the present study, we focused on mRNA expression, immunochemical localization, and externalization of galectin-1 in mature DRG and peripheral nerves. *In situ* hybridization and immunohistochemistry (Figs 2 and 3A) revealed an intense expression of galectin-1 in DRG neurons with smaller diameters, which was in agreement with previous findings (Regan *et al.*, 1986; Hynes *et al.*, 1990). There may be a discrepancy between the findings from *in situ* hybridization and those from immunohistochemistry: mRNA expression, but not immunoreactivity for galectin-1, was detected in larger neurons. The immunohistochemistry on DRG sections (Fig. 3A) was carried out with antigalectin-1 antibody, which was diluted to 1 : 1000 with 0.5% skimmed milk. However, the immunohistochemistry with higher concentration of the antibody (1 : 200–1 : 300) resulted in weak but visible immunoreactivity for galectin-1 in larger neurons (K. Sang and K. Ajiki, unpublished observations). This result was consistent with that of our previous study (Fukaya *et al.*, 2003), in which the antibody was diluted 1 : 100 prior to use. Taking these findings into consideration, galectin-1 is likely to be synthesized in and distributed to all DRG neurons. Also, it is obvious from those studies that both mRNA expression and immunoreactivity for this lectin in smaller neurons are much more intense than those in larger neurons in intact DRG. The small neurons were reported to have small axonal fibres such as Aδ and C, which can play an essential role in mechanical and polymodal nociception (Salt & Hill, 1983). Therefore, cytosolic galectin-1 in small DRG neurons may be involved in such small-fibre functions. A recent study by Senba *et al.* (2001) revealed that most of galectin-1-immunoreactive DRG neurons expressed mRNA for c-ret but not for trkA. Because c-ret and trkA are proto-oncogenes of the functional receptors for glial cell line-derived neurotrophic factor (GDNF) and nerve growth factor (NGF), respectively (Kashiba *et al.*, 1998), this finding suggests that galectin-1 is expressed in GDNF-responsive DRG neurons rather than NGF-responsive neurons. Regan *et al.* (1986) observed intense immunoreactivity for galectin-1 in the central processes of DRG neurons (i.e. dorsal funiculus and dorsal horn) in embryonic and neonatal rats, but the immunoreactiv was decreased and restricted to the superficial dorsal horn in adult rats. In contrast, Senba *et al.* (2001) showed axotomy-induced up-regulation of galectin-1 in the dorsal horn of adult rats, suggesting a role for endogenous galectin-1 in the pathological pain due to nerve injury. By RT-PCR analysis (Fig. 1), galectin-1 mRNA was detected in both ganglia and spinal nerve fibres. Because the latter do not contain neuronal cell bodies, this finding suggests that galectin-1 can be synthesized in non-neuronal cells of nerve fibres. Although it was difficult to conclude the expression of galectin-1 mRNA in non-neuronal cells by *in situ* hybridization (Fig. 2), immunohistochemistry showed that Schwann cells within the spinal nerve sections were intensely stained with the galectin-1 antibody (Fig. 3A). This is consistent with previous findings using sections of rat sciatic nerves (Fukaya *et al.*, 2003). Taking the results of RT-PCR and immunohistochemistry together, it appears likely that galectin-1 is synthesized in Schwann cells. Consistently, Northern blot analysis (Fig. 5B) showed galectin-1 mRNA expression in the spontaneously immortalized adult mouse Schwann cells (IMS32).

In contrast to the studies *in vivo*, galectin-1 immunoreactivity was observed in almost all DRG neurons from a very early stage (3 h)

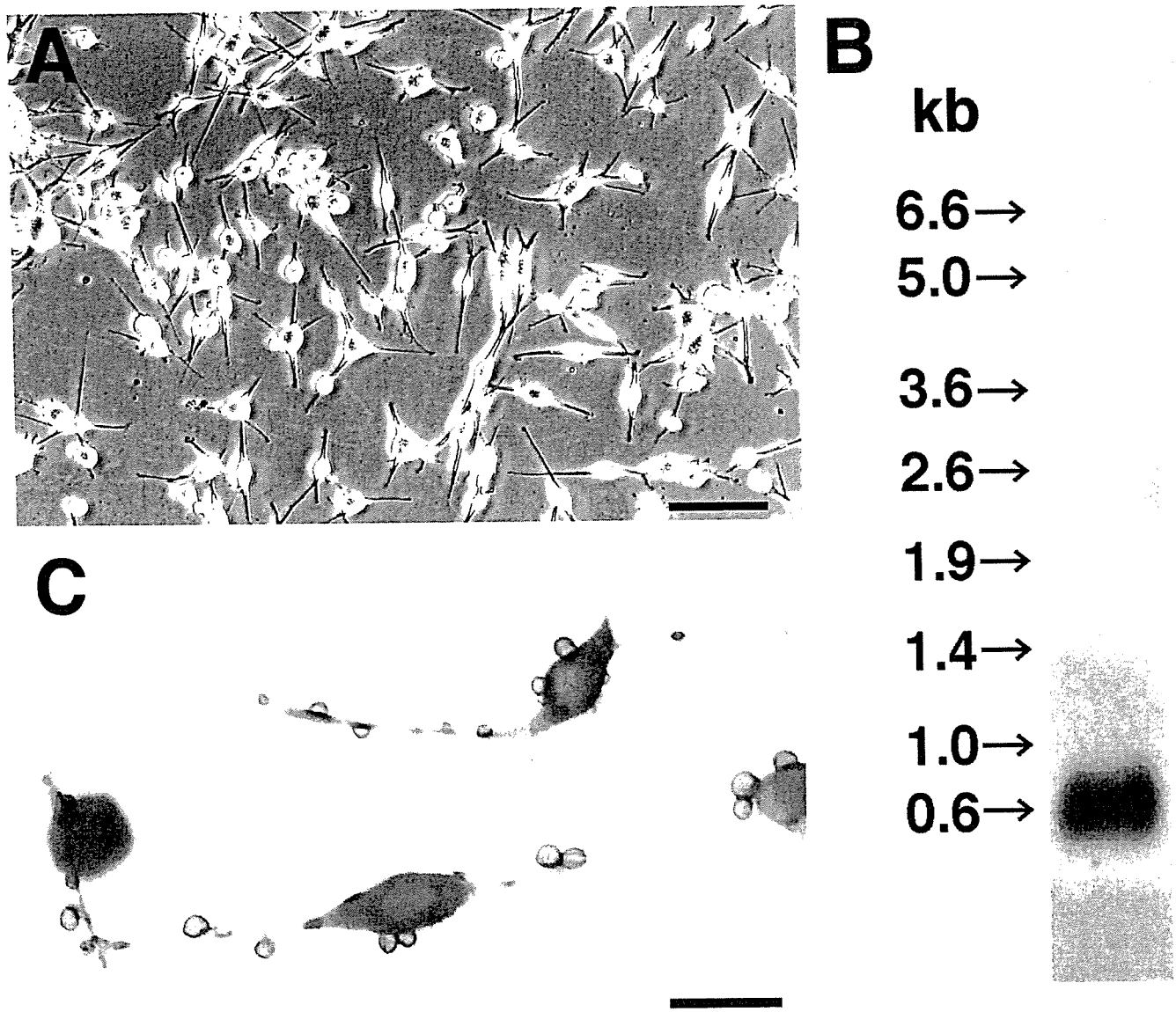

FIG. 5. Expression of galectin-1 in immortalized adult mouse Schwann cells (IMS32). (A) A phase-contrast micrograph of IMS32 cells. (B) Northern blot analysis of IMS32 cell mRNAs. After transfer, the bound mRNAs were hybridized with a 408-bp rat galectin-1 cDNA probe labelled with AlkPhos Direct (Amersham Biosciences). Marker molecular masses for calibration are indicated on the left. (C) Immunocytochemical localization of galectin-1 in IMS32 cells. Intense immunoreaction with vesicular shapes was observed on the cell surface protruding to an extracellular space, suggesting the externalization of galectin-1 from the cells. Scale bars, 50 μm (A), 10 μm (C).

culture (Fig. 3B). Enzymatic and mechanical treatments for the dissociation of DRG cells, together with disruption of the interactions between neurons and satellite cells, are detrimental to the survival of neurons, and some neurons die during *in vivo–in vitro* replacement (Sango *et al.*, 1991, 2003; Kasper *et al.*, 1999). Therefore, galectin-1 expressed in cultured DRG neurons may play a role in the repair of neurons from injury caused by the dissociation procedure and/or protection of neurons from death at the initial phase in culture. As the culture time increased, galectin-1 immunoreactivity became concentrated at the surface of neurons (Fig. 3C–E). In addition, Schwann cells proliferated and began to express galectin-1 at later stages in culture (Fig. 3E). At a higher magnification, the immunoreactivity for galectin-1 was visualized as vesicles budding off the surface of Schwann cells (Fig. 3F). These light microscopic findings were consistent with the results of immunoelectron microscopy (Fig. 6) and indicate the extracellular release of galectin-1 from neurons and Schwann cells in culture. This was further confirmed by Western blot analysis: both reduced and oxidized forms of galectin-1 were detected in the culture media of DRG neurons (Fig. 7, lower panel) and IMS32 cells (Fig. 7, upper panel) under nonreducing conditions. The immunoreactivity for galectin-1 in the medium of DRG neurons was much lower than that in the medium of IMS32 cells, which may be because the culture medium was initially collected at 48 h after seeding. Immunocytochemical studies showed localization of galectin-1 on the surface of DRG neurons beyond 2 days in culture, suggesting that the extracellular release of this molecule may be increased at later stages of culture. In contrast, the surface and extracellular immunoreactivities for galectin-1 were observed in IMS32 cells at all observation periods, from 1 to 4 days after seeding. Thus, it appears that IMS32 cells constantly synthesize and secrete galectin-1 regardless of incubation time. IMS32 cells have been established from long-term cultures of adult mouse DRG and peripheral nerves (Watabe *et al.*, 1995).

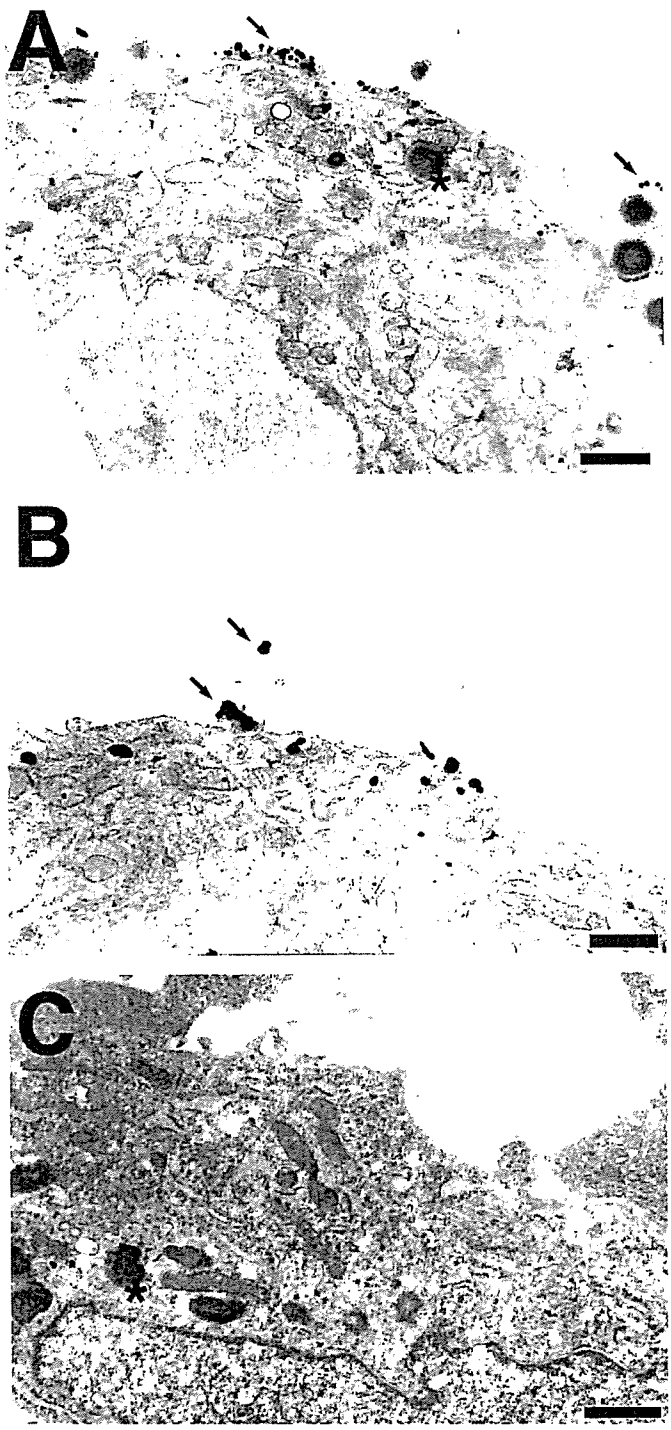

FIG. 6. Electron micrographs of (A) adult rat DRG neurons and (B) IMS32 cells, stained with an antibody to galectin-1. Cells at 7 days after seeding were processed for immunocytochemistry and embedded in epoxy resin. The immunogold particles (indicated as arrows in A and B) were found mainly at the cell periphery and/or outside the cell soma. (C) Substitution of the primary antibody with preimmune rabbit IgG resulted in no staining. The intracellular electron dense materials (indicated as asterisks in A and C) appeared to be lysosomes. cale bars, 1 μm (A), 0.5 μm (B), 0.7 μm (C).

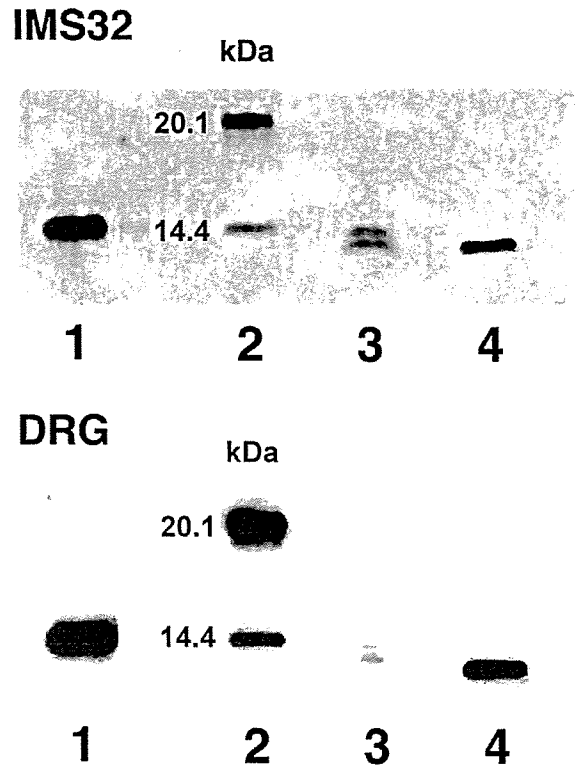

FIG. 7. Western blot analysis of culture medium obtained from IMS32 cells (upper panel) and DRG neurons (lower panel) for galectin-1. Oxidized recombinant human galectin-1 (2 ng) (lanes 1 and 4) and the culture supernatant of IMS32 cells (lane 3, upper panel) and DRG neurons (lane 3, lower panel) were analysed by SDS–PAGE on a 15–25% gradient gel in the presence (lane 1) or absence (lanes 3 and 4) of 20 mM dithiothreitol. Immunocomplexes on the blotted membrane were visualized by chemiluminesence using an image analyser. Molecular size markers are shown in lane 2.

These cells showed distinct Schwann cell phenotypes as described in Results, as well as in previous reports (Watabe *et al.*, 1995, 2003). Although IMS32 cells are different from primary and long-term cultured Schwann cells in that the former were not contact-inhibited and formed ball-shaped subcolonies when cultures reached confluence, IMS32 cells exhibit mitogenic responses to several growth factors [e.g. platelet-derived growth factor (PDGF)-BB, acidic and basic fibroblast growth factor (aFGF, bFGF), transforming growth factor (TGF)-β1,2] which were similar to primary and long-term cultured Schwann cells (Watabe *et al.*, 1994). Immunocytochemistry on IMS32 cells and primary-cultured Schwann cells which were kept in the same culture media (i.e. DMEM or F12 in the presence or absence of serum) revealed that the former showed more intense cytosolic immunoreactivity for galectin-1 with more extensive vesicle formation outside the cell soma than did the latter, under any culture conditions (not shown). These findings imply that IMS32 cells could produce and externalize higher amounts of galectin-1 than primary-cultured Schwann cells, regardless of components of the culture medium. The detection of both reduced and oxidized forms of galectin-1 suggested that some galectin-1 molecules externalized from DRG neurons or IMS32 cells were oxidized. The physiological extracellular environment appears to be oxidative, and injury-induced nitric oxide (NO) in the extracellular space may accelerate the oxidization of galectin-1 (Guizar-Sahagun *et al.*, 1998). However, it remains possible that oxidization of the molecule takes place during electrophoresis without a reducing agent. We are currently trying to develop a monoclonal antibody which could specifically recognize the oxidized form of galectin-1. Such an antibody would be helpful in obtaining more precise information about the form of galectin-1 on the cell surface and in the extracellular space.

Galectin-1 is not a typical secreted protein because cDNA sequences of galectin-1 lack a recognizable secretion signal (Clerch *et al.*, 1988; Wilson *et al.*, 1989). Based on the findings from immunocytochemical studies with myogenic cells, Cooper & Barondes (1990) hypothesized a 'nonclassical' pathway for its secretion as follows. Galectin-1, initially distributed throughout the cytosol, becomes concentrated in the cytoplasm beneath the plasma membrane (ectoplasm), accumulates in restricted regions of ectoplasm and evaginates to form extracellular vesicles. Subsequent disruption of the evaginated vesicles results in a release of the lectin into the extracellular milieu. This hypothesis is supported by findings from previous studies which used several cell lines (Avellana-Adalid *et al.*, 1994; Cho & Cummings, 1995; Lutomski *et al.*, 1997) and the present study with DRG neurons and Schwann cells. The externalization of galectin-1 accompanies differentiation of myoblasts (Cooper & Barondes, 1990) and leukaemia cell lines (Lutomski *et al.*, 1997), whereas induction of neuroblastoma differentiation markedly decreased its externalization (Avellana-Adalid *et al.*, 1994). These findings imply that galectin-1 secretion is tightly controlled during development and differentiation (Hughes, 1999). In contrast, the results in the present study suggest its release from DRG neurons and Schwann cells of adult animals in culture. Because some biological properties of these cells change with postnatal development and maturation (Lindsay, 1988; Horie *et al.*, 1990; Chi *et al.*, 1993), it appears that the culture system of adult DRG is useful for the study of plasticity and regeneration of the peripheral nervous system (Sango *et al.*, 2003). The nonclassical pathway for the secretion of galectin-1 shown in neurons and Schwann cells *in vitro* may be, at least partially, applicable to these cells *in vivo*. In fact, intense immunoreactivity for galectin-1 was observed in the axons and Schwann cells which had regenerated or migrated into a grafted silicone tube after transection of adult rat peroneal nerves (Horie *et al.*, 1999). Therefore, cytosolic galectin-1 is likely to be released from growing axons and Schwann cells into the extracellular space upon axonal injury. Galectin-1 is distributed to both neuronal cell bodies and axons in intact peripheral nerves (Horie *et al.*, 1999; Fukaya *et al.*, 2003), suggesting that the lectin molecules synthesized in the cell soma are transported to the axon terminals (Kitchener *et al.*, 1994). However, it should be noted that in this study the immunoreactivity for galectin-1 was localized at the cell soma, not at the neurites of DRG neurons in culture in the absence of serum (Fig. 4A–C). In contrast, the intense immunoreactivity was detected in both neuronal cell bodies and neurites in culture in the presence of serum (Fig. 4D–F). The latter finding is consistent with that *in vivo* and suggests galectin-1 transport from the neuronal cell bodies to the neurites. It is recognized that neurons kept in serum-containing medium could survive and extend neurites better than those kept in serum-free medium (Oorschot & Jones, 1986; Sango *et al.*, 1991; Sotelo *et al.*, 1991). This suggests that survival and neurite formation of cultured neurons could be promoted by known and unknown factors contained in serum. Similarly, it appears that some molecules in serum could facilitate synthesis and/or axonal transport of galectin-1 in DRG neurons. On the other hand, most of the cultures were kept in serum-free medium in this study in order to avoid the effects of serum-derived factors on the extracellular expressions of galectin-1.

It is possible that galectin-1 released from neurons and Schwann cells acts on peripheral nervous tissues in an autocrine fashion. Many studies have suggested functional significance of galectin-1 in the reduced form during neural development and regeneration. For example, recombinant reduced galectin-1, when used as a coating substrate, promoted adhesion, aggregation and neurite fasciculation of neonatal rat DRG neurons (Outenreath & Jones, 1992) and olfactory neurons (Mahanthappa *et al.*, 1994; Puche *et al.*, 1996). On the other hand, little attention has been paid to the oxidized form, which was considered to lack biological activities. Our recent findings shed light on oxidized galectin-1 as a novel neurotrophic molecule for mature sensory and motor neurons: recombinant human oxidized galectin-1 stimulated axonal regeneration and Schwann cell migration from the transected nerve stumps *in vivo* (Horie *et al.*, 1999; Fukaya *et al.*, 2003) and *in vitro* (Inagaki *et al.*, 2000). Because oxidized galectin-1 enhanced neurite outgrowth from transected nerve terminals of DRG explants but not from dissociated DRG neurons (Horie *et al.*, 1999), it is likely to stimulate non-neuronal cells to initiate axonal regeneration rather than act directly on neurons. Further studies are needed to clarify the action mechanisms of oxidized galectin-1 for the promotion of neural regeneration.

In summary, the results in the present study suggest that galectin-1 is externalized from neurons and Schwann cells of mature DRG *in vitro*. Some of the galectin-1 molecules in the extracellular space may be converted to the oxidized form, which loses lectin activity but displays neurotrophic function as a cytokine-like molecule. Due to its potent activity on neural regeneration, oxidized galectin-1 may play a pivotal role in restoration of peripheral nerve lesions caused by trauma and surgical operation (Horie & Kadoya, 2000; Fukaya *et al.*, 2003).

Acknowledgements

This study was supported by a Grant-in-aid for Scientific Research, from the Ministry of Education, Science, Sports and Culture, Japan, and by Funds from Mitsui Life Social Welfare Foundation and Suzuken Memorial Foundation. We thank Drs Yusaku Nakabeppu, Emiko Senba, Soroku Yagihashi and Hitoshi Yasuda for helpful suggestions and Dr Miwa Sango-Hirade for the help preparing figures.

Abbreviations

CHO (cells), Chinese hamster ovary (cells); DRG, dorsal root ganglia; PBS, phosphate-buffered saline; RT-PCR, reverse transcription–polymerase chain reaction.

References

Avellana-Adalid, V., Rebel, G., Caron, M., Cornillot, J.-D., Bladier, D. & Joubert-Caron, R. (1994) Changes in S-type lectin localization in neuroblastoma cells (NIE115) upon differentiation. *Glycoconjugate J.*, **11**, 286–291.

Barondes, S.H., Castronovo, V., Cooper, D.N.W., Cummings, R.D., Drickamer, K., Feizi, T., Gitt, M.A., Hirabayashi, J., Hughes, C., Kasai, K., Leffler, H., Liu, F., Lotan, R., Mercurio, A.M., Monsigny, M., Pillai, S., Poirer, F., Raz, A., Rigby, P.W.J. & Wang, J.L. (1994) Galectins; a family of animal β-galactoside-binding lectins. *Cell*, **76**, 597–598.

Camby, I., Belot, N., Rorive, S., Lefranc, F., Maurage, C.A., Lahm, H., Kaltner, H., Hadari, Y., Ruchoux, M.M., Brotchi, J., Zick, Y., Salmon, I., Gabius, H.J. & Kiss, R. (2001) Galectins are differentially expressed in supratentorial pilocytic astrocytomas, astrocytomas, anaplastic astrocytomas and glioblastomas, and significantly modulate tumor astrocyte migration. *Brain Pathol.*, **11**, 12–26.

Chi, H., Horie, H., Hikawa, N. & Takenaka, T. (1993) Isolation and age-related characterization of mouse Schwann cells from dorsal root ganglion explants in type I collagen gels. *J. Neurosci. Res.*, **35**, 183–187.

Cho, M. & Cummings, R.D. (1995) Galectin-1, a β-galactoside-binding lectin in Chinese hamster ovary cells. *J. Biol. Chem.*, **270**, 5207–5212.

Clerch, L.B., Whitney, P., Hass, M., Brew, K., Miller, T., Werner, R. & Massaro, D. (1988) Sequence of a full-length cDNA for rat lung β-galactoside-binding protein: primary and secondary structure of the lectin. *Biochemistry*, **27**, 692–699.

Cleves, A.E., Cooper, D.N.W., Barondes, S.H. & Kelly, R.B. (1996) A new pathway for protein export in *Saccharomyces cerevisiae*. *J. Cell Biol.*, **133**, 1017–1026.

Cooper, D.N.W. & Barondes, S.H. (1990) Evidence for export of a muscle lectin from cytosol to extracellular matrix and for a novel secretory mechanism. *J. Cell Biol.*, **110**, 1681–1691.

Cooper, D.N.W. & Barondes, S.H. (1999) God must love galectins; he made so many of them. *Glycobiology*, **9**, 979–984.

Danielsen, E.M. & van Deurs, B. (1997) Galectin-4 and small intestinal brush border enzymes from clusters. *Mol. Biol. Cell*, **8**, 2241–2251.

Fukaya, K., Hasegawa, M., Kadoya, T., Horie, H., Fujisawa, H., Hayashi, Y., Tachibana, O., Kida, S. & Yamashita, J. (2003) Oxidized galectin-1 stimulates the migration of Schwann cells from both proximal and distal stumps of transected nerves and promotes axonal regeneration after peripheral nerve injury. *J. Neuropathol. Exp. Neurol.*, **62**, 162–172.

Guizar-Sahagun, G., Garcia-Lopez, P., Espitia, A.L., Grijalva, I., Franco-Bourland, R.E. & Madrazo, I. (1998) Transitory expression of NAPDH diaphorase (NOS) in axonal swellings after spinal cord injury. *Neuroreport*, **9**, 2899–2902.

Horie, H., Ikuta, S. & Takenaka, T. (1990) Membrane elasticity of mouse dorsal root ganglion neurons decreases with aging. *FEBS Lett.*, **269**, 23–25.

Horie, H., Inagaki, Y., Sohma, Y., Nozawa, R., Okawa, K., Hasegawa, M., Muramatsu, N., Kawano, H., Horie, M., Koyama, H., Sakai, I., Takeshita, K., Kowada, Y., Takano, M. & Kadoya, T. (1999) Galectin-1 regulates initial axonal growth in peripheral nerves after axotomy. *J. Neurosci.*, **19**, 9964–9974.

Horie, H. & Kadoya, T. (2000) Identification of oxidized galectin-1 as an initial repair regulatory factor after axotomy in peripheral nerves. *Neurosci. Res.*, **38**, 131–137.

Hughes, R.C. (1999) Secretion of the galectin family of mammalian carbohydrate-binding proteins. *Biochem. Biophys. Acta*, **1473**, 172–185.

Hynes, M.A., Gitt, M., Barondes, S.H., Jessell, T.M. & Buck, L.B. (1990) Selective expression of an endogenous lactose-binding lectin gene in subsets of central and peripheral neurons. *J. Neurosci.*, **10**, 1004–1013.

Ichikawa, T., Ajiki, K., Matsuura, J. & Misawa, H. (1997) Localization of two cholinergic markers, choline acetyltransferase and vesicular acetylcholine transporter in the central nervous system of the rat: in situ hybridization histochemistry and immunohistochemistry. *J. Chem. Neuroanat.*, **13**, 23–39.

Inagaki, Y., Sohma, Y., Horie, H., Nozawa, R. & Kadoya, T. (2000) Oxidized galectin-1 promotes axonal regeneration in peripheral nerves but does not possess lectin properties. *Eur. J. Biochem.*, **267**, 2955–2964.

Kasai, K. & Hirabayashi, J. (1996) Galectins: a family of animal lectins that decipher glycocodes. *J. Biochem.*, **119**, 1–8.

Kashiba, H., Hyon, B. & Senba, E. (1998) Glial cell line-derived neurotrophic factor and nerve growth factor receptor mRNAs are expressed in distinct subgroups of dorsal root ganglion neurons and are differentially regulated by peripheral axotomy in the rat. *Neurosci. Lett.*, **252**, 107–110.

Kasper, M., Tonge, D. & Gordon-Weeks, P.R. (1999) Regeneration of adult dorsal root ganglion axons in explant culture. In Haynes, L.W. (ed.), *The Neuron in Tissue Culture*. John Wiley & Sons Ltd, Chichester, pp. 74–86.

Kawano, H., Fukuda, T., Kubo, K., Horie, M., Uyemura, K., Takeuchi, K., Osumi, N., Eto, K. & Kawamura, K. (1999) Pax-6 is required for thalamocortical pathway formation in fetal rats. *J. Comp. Neurol.*, **408**, 147–160.

Kitchener, P.D., Wilson, P. & Snow, P.J. (1994) Sciatic axotomy compromises axonal transport of transganglionic tracer BSI-B4 from the soma to the central terminals of C fibre afferents. *Neurosci. Lett.*, **166**, 121–125.

Lahm, H., Andre, S., Hoeflich, A., Fischer, J.R., Sordat, B., Kaltner, H., Wolf, E. & Gabius, H.J. (2001) Comprehensive galectin fingerprinting in a panel of 61 human tumor cell lines by RT-PCR and its implications for diagnostic and therapeutic procedures. *J. Cancer Res. Clin. Oncol.*, **127**, 375–386.

Lindsay, R.M. (1988) Nerve growth factors (NGF, BDNF) enhance axonal regeneration but are not required for survival of adult sensory neurons. *J. Neurosci.*, **8**, 2394–2405.

Llewellyn-Smith, I.J., Costa, M. & Furness, J.B. (1985) Light and electron microscopic immunocytochemistry of the same nerves from whole mount preparations. *J. Histochem. Cytochem.*, **33**, 857–866.

Lutomski, D., Fouillit, M., Bourin, P., Mellottee, D., Denize, N., Pontet, M., Bladier, D., Caron, M. & Joubert-Caron, R. (1997) Externalization and binding of galectin-1 on cell surface of K562 cells upon erythroid differentiation. *Glycobiology*, **7**, 1193–1199.

Mahanthappa, N.K., Cooper, D.N.W., Barondes, S.H. & Schwarting, G.A. (1994) Rat olfactory neurons can utilize the endogenous lectin, L-14, in a novel adhesion mechanism. *Development*, **120**, 1373–1384.

Mehul, B. & Hughes, R.C. (1997) Plasma membrane targetting, vesicular budding and release of galectin 3 from the cytoplasm of mammalian cells during secretion. *J. Cell Sci.*, **110**, 1169–1178.

Oorschot, D.E. & Jones, D.G. (1986) Tissue culture analysis of neurite outgrowth in the presence and absence of serum: possible relevance for central nervous system regeneration. *J. Neurosci. Res.*, **15**, 341–352.

Outenreath, R.L. & Jones, A.L. (1992) Influence of an endogenous lectin substrate on cultured dorsal root ganglion cells. *J. Neurocytol.*, **21**, 788–795.

Perillo, N.L., Marcus, M.E. & Baum, L.G. (1998) Galectins: versatile modulators of cell adhesion, cell proliferation, and cell death. *J. Mol. Med.*, **76**, 402–412.

Perillo, N.L., Pace, K.E., Seihamer, J.L. & Baum, L.G. (1995) Apoptosis of T-cells mediated by galectin-1. *Nature*, **378**, 736–739.

Pesheva, P., Kuklinski, S., Schmitz, B. & Probstmeier, R. (1998) Galectin-3 promotes neural cell adhesion and neurite growth. *J. Neurosci. Res.*, **54**, 639–654.

Puche, A.C., Poirier, F., Hair, M., Bartlett, P.F. & Key, B. (1996) Role of galectin-1 in the developing mouse olfactory system. *Dev. Biol.*, **179**, 274–287.

Rabinovich, G.A., Alonso, C.R., Sotomayor, C.E., Durand, S., Bocco, J.L. & Riera, C.M. (2000a) Molecular mechanisms implicated in galectin-1-induced apoptosis: activation of the AP-1 transcription factor and downregulation of Bcl-2. *Cell Death Differ.*, **7**, 747–753.

Rabinovich, G.A., Baum, L.G., Tinari, N., Paganelli, R., Natoli, C., Liu, F.T. & Iacobelli, S. (2002) Galectins and their ligands: amplifiers, silencers or tuners of the inflammatory response? *Trends Immunol.*, **23**, 313–320.

Rabinovich, G.A., Sotomayor, C.E., Riera, C.M., Bianco, I. & Correa, S.G. (2000b) Evidence of a role for galectin-1 in acute inflammation. *Eur. J. Immunol.*, **30**, 1331–1339.

Regan, L.J., Dodd, J., Barondes, S.H. & Jessell, T.M. (1986) Selective expression of endogenous lactose-binding lectins and lactoseries glycoconjugates in subsets of rat sensory neurons. *Proc. Natl. Acad. Sci. USA*, **83**, 2248–2252.

Salt, T.E. & Hill, R.G. (1983) Neurotransmitter candidates of somatosensory primary afferent fibers. *Neuroscience*, **10**, 1083–1103.

Sango, K., Horie, H., Saito, H., Ajiki, K., Tokashiki, A., Takeshita, K., Ishigatsubo, Y., Kawano, H. & Ishikawa, Y. (2002b) Diabetes is not a potent inducer of neuronal cell death in mouse sensory ganglia, but it enhances neurite regeneration in vitro. *Life Sci.*, **71**, 2351–2368.

Sango, K., Horie, H., Sotelo, J.R. & Takenaka, T. (1991) A high glucose environment improves survival of diabetic neurons in culture. *Neurosci. Lett.*, **129**, 277–280.

Sango, K., Oohira, A., Ajiki, K., Tokashiki, A., Horie, M. & Kawano, H. (2003) Phosphacan and neurocan are repulsive substrata for adhesion and neurite extension of adult rat dorsal root ganglion neurons *in vitro*. *Exp. Neurol.*, **182**, 1–11.

Sango, K., Yamanaka, S., Ajiki, K., Tokashiki, A. & Watabe, K. (2002a) Lysosomal storage results in impaired survival but normal neurite outgrowth in dorsal root ganglion neurons from a mouse model of Sandhoff disease. *Neuropathol. Appl. Neurobiol.*, **28**, 23–34.

Senba, E., Imbe, H., Kami, K. & Morikawa, Y. (2001) Expression and functions of Galectin-1 in injured afferent system and muscles. *Neurosci. Res. Suppl.*, **25**, S30–4.

Sotelo, J.R., Horie, H., Ito, S., Benech, C., Sango, K. & Takenaka, T. (1991) An in vitro model to study diabetic neuropathy. *Neurosci. Lett.*, **129**, 91–94.

Toba, Y., Horie, M., Sango, K., Tokashiki, A., Matsui, F., Oohira, A. & Kawano, H. (2002) Expression and immunohistochemical localization of heparan sulfate proteoglycan N-syndecan in the migratory pathway from the rat olfactory placode. *Eur. J. Neurosci.*, **15**, 1461–1473.

Tracey, B.M., Feizi, T., Abbott, W.M., Carruthers, R.A., Green, B.N. & Lawso A.M. (1992) Subunit molecular mass assignment of 14,654 Da to the solub beta-galactoside-binding lectin from bovine heart muscle and demonstration of intramolecular disulfide bonding associated with oxidative inactivation. *J. Biol. Chem.*, **267**, 10342–10347.

de Waard, A., Hickman, S. & Kornfeld, S. (1976) Isolation and properties of beta-galactoside binding lectins of calf heart and lung. *J. Biol. Chem.*, **251**, 7581–7587.

Watabe, K., Fukuda, T., Tanaka, J., Honda, H., Toyohara, K. & Sakai, O. (1995) Spontaneously immortalized adult mouse Schwann cells secrete autocrine and paracrine growth-promoting activities. *J. Neurosci. Res.*, **41**, 279–290.

Watabe, K., Fukuda, T., Tanaka, J., Toyohara, K. & Sakai, O. (1994) Mitogenic effects of platelet-derived growth factor, fibroblast growth factor, transforming growth factor-β, and heparin-binding serum factor for adult mouse Schwann cells. *J. Neurosci. Res.*, **39**, 525–534.

Watabe, K., Sakamoto, T., Kawazoe, Y., Michikawa, M., Miyamoto, K., Yamamura, T., Saya, H. & Araki, N. (2003) Tissue culture methods to study neurological disorders: Establishment of immortalized Schwann cells from murine disease models. *Neuropathology*, **23**, 68–78.

Wilson, T.J.G., Firth, M.N., Powell, J.T. & Harrison, F.L. (1989) The sequence of the 14 kDa β-galactoside-binding lectin and evidence for its synthesis on free cytoplasmic ribosomes. *Biochem. J.*, **261**, 847–852.

Zajc Kreft, K., Kreft, S., Komel, R. & Grubic, Z. (2000) Nonradioactive northern blotting for the determination of acetylcholinesterase mRNA. Comparison to the radioactive technique. *Pflugers Arch.*, **439** (Suppl.), R66–R67.

Gene Therapy (2004) 11, 784–790

www.nature.com/gt

RESEARCH ARTICLE

Postischemic administration of Sendai virus vector carrying neurotrophic factor genes prevents delayed neuronal death in gerbils

M Shirakura[1,2], M Inoue[1], S Fujikawa[1], K Washizawa[1], S Komaba[1], M Maeda[3], K Watabe[4], Y Yoshikawa[2] and M Hasegawa[1]

[1]*DNAVEC Research Inc., Tsukuba, Japan;* [2]*Department of Biomedical Science, Graduate School of Agricultural and Life Sciences, University of Tokyo, Tokyo, Japan;* [3]*First Department of Anatomy, Osaka City University Medical School, Osaka, Japan; and* [4]*Department of Molecular Neuropathology, Tokyo Metropolitan Institute for Neuroscience, Tokyo, Japan*

Sendai virus (SeV) vector-mediated gene delivery of glial cell line-derived neurotrophic factor (GDNF) and nerve growth factor (NGF) prevented the delayed neuronal death induced by transient global ischemia in gerbils, even when the vector was administered several hours after ischemia. Intraventricular administration of SeV vector directed high-level expression of the vector-encoded neurotrophic factor genes, which are potent candidates for the treatment of neurodegenerative diseases. After occlusion of the bilateral carotid arteries of gerbils, SeV vector carrying GDNF (SeV/GDNF), NGF (SeV/NGF), brain-derived neurotrophic factor (SeV/BDNF), insulin-like growth factor-1 (SeV/IGF-1) or vascular endothelial growth factor (SeV/VEGF) was injected into the lateral ventricle. Administration of SeV/GDNF, SeV/NGF or SeV/BDNF 30 min after the ischemic insult effectively prevented the delayed neuronal death of the hippocampal CA1 pyramidal neurons. Furthermore, the administration of SeV/GDNF or SeV/NGF as late as 4 or 6 h after the ischemic insult also prevented the death of these neurons. These results indicate that SeV vector-mediated gene transfer of neurotrophic factors has high therapeutic potency for preventing the delayed neuronal death induced by transient global ischemia, and provides an approach for gene therapy of stroke.

Gene Therapy (2004) **11,** 784–790. doi:10.1038/sj.gt.3302224
Published online 12 February 2004

Keywords: *Sendai virus; cerebral ischemia; delayed neuronal death; GDNF; NGF*

Neurons are postmitotic and highly differentiated, and are extremely vulnerable to ischemic injury. Pyramidal cells of the hippocampal CA1 region are well known to be especially vulnerable to cerebral ischemia.[1,2] Neuronal cell death in the CA1 region itself is not death-dealing but results in severe deficits of memory function.[3–5] Since the regeneration of neuronal cells remains critically difficult at present, protection against the neuronal loss induced by ischemic injury is vital in cerebrovascular-type dementia.

Glial cell line-derived neurotrophic factor (GDNF) is a potent neurotrophic factor that promotes the cell survival and differentiation of dopaminergic neurons[6,7] and motoneurons.[8,9] Nerve growth factor (NGF) also has a potent ability to protect neurons from various injuries and promote the survival of cholinergic neurons.[10–12] These neurotrophic factors may be valuable as candidates for use in therapy of neurodegenerative diseases. It has been reported that the neuronal cell death induced by ischemic injury was prevented by the administration of GDNF[13–15] and NGF[16–18] proteins. However, the usefulness of such protein factors in patients is limited because of their poor bioavailability and short half-lives. Moreover, these agents might be ineffective without direct injection and continuous infusion into the ventricle, striatum or cerebral cortex. Therefore, virus vector-mediated gene transfer is expected to be an effective approach for the delivery of therapeutic proteins into the central nervous system (CNS). Even in the case of unsustained, but transient, expression by the vectors, it would enable significant cutting down of the number of required administrations. Previous studies demonstrated that gene transfer of neurotrophic factors such as GDNF[19] and NGF[20,21] rescued neuronal cells from ischemic injury in animal models. However, there have not been any reports in which neurotrophic factors expressed using conventional vectors such as adenovirus, retrovirus or adeno-associated virus were shown to promote the survival of neurons when the vectors were administered after ischemia.

We have developed a new type of gene transfer vector using Sendai virus (SeV), which is classified as a type I parainfluenza virus belonging to the family *Paramyxoviridae* with a negative-strand RNA genome.[22,23] SeV has a strictly cytoplasmic life cycle in mammalian cells, that is, its genomic RNA is restricted to the cytoplasm and has no interaction with the host chromosomes.[22] Therefore, SeV vector causes no genotoxicity such as the permanent integration in the target cells sometimes observed with other conventional viral

Correspondence: M Inoue, 1-25-11 Kannondai, Tsukuba-shi, Ibaraki 305-0856, Japan
Received 16 May 2003; accepted 29 November 2003; published online 12 February 2004

vectors. SeV has the ability to infect most mammalian cells such as neuronal and muscular cells and directs high-level gene expression in these cells.[23–26] Indeed, we observed potent infectivity of SeV vector in ependymal cells after intraventricular administration in the CNS.[27] When the SeV vector carrying enhanced green fluorescent protein gene (SeV/GFP) was administered into the left lateral ventricle of gerbils, intense GFP expression was observed around the ependymal layer of the lateral ventricles (Figure 1c) and around the hippocampus (Figure 1b). Immunohistochemical analysis using anti-SeV antibody clearly showed that the cells supporting SeV replication were ependymal cells in the lateral ventricles (Figure 1d), third ventricle (Figure 1e) and around the hippocampus (Figure 1f). We previously showed that SeV vector-mediated gene transfer of GDNF 4 days before transient ischemia prevented the delayed neuronal death induced by transient global ischemia in gerbils.[27] However, SeV vector was administered prior to the ischemic insult in that case, too, whereas gene therapy must be applied after the occurrence of a stroke for clinical application. In the present study, we examined the effects of postischemic administration of SeV vectors carrying GDNF, NGF and other neurotrophic factor genes on the delayed neuronal death induced by transient global ischemia. Our results suggest that SeV vector-mediated gene transfer has a therapeutic high potential for cerebral ischemia.

In order to confirm the efficient gene transfer and expression of SeV in the CNS, the proteins derived from the genes harbored in the SeV vector were quantified. SeV vectors such as SeV/GDNF, SeV/NGF and SeV/GFP were administered into the left lateral ventricle of gerbils at 5×10^6 PFU/head, and the amount of GDNF and NGF proteins in the hippocampus was quantified by ELISA assays. High-level expression of GDNF (114 ± 6 pg/mg tissue) and NGF (1130 ± 60 pg/mg tissue) proteins was detected in the hippocampus of gerbils as early as 1 day after injection of SeV/GDNF and SeV/NGF, respectively (Figure 2a, b). In contrast, only a very small amount of GDNF or NGF protein was detected when the gerbils were treated with SeV/GFP. The expression of GDNF (2340 ± 200 pg/mg tissue) and NGF (3360 ± 290 pg/mg tissue) proteins reached peak levels 4 days after injection of SeV/GDNF and SeV/NGF, respectively, and then returned to the original level 14 days after the injection. In another experiment, an increment of GDNF expression in the cerebrospinal fluid was detected 8 h after injection of SeV/GDNF (data not shown). These results indicate that rapid and high-level expression of neurotrophic factors can be achieved by the administration of SeV vectors in the CNS. Also, the expression level achieved using SeV vectors was remarkably high compared with that achieved using adenovirus. For example, the GDNF concentration was reported to be 2.2 ± 0.5 pg/mg tissue 1 day after the

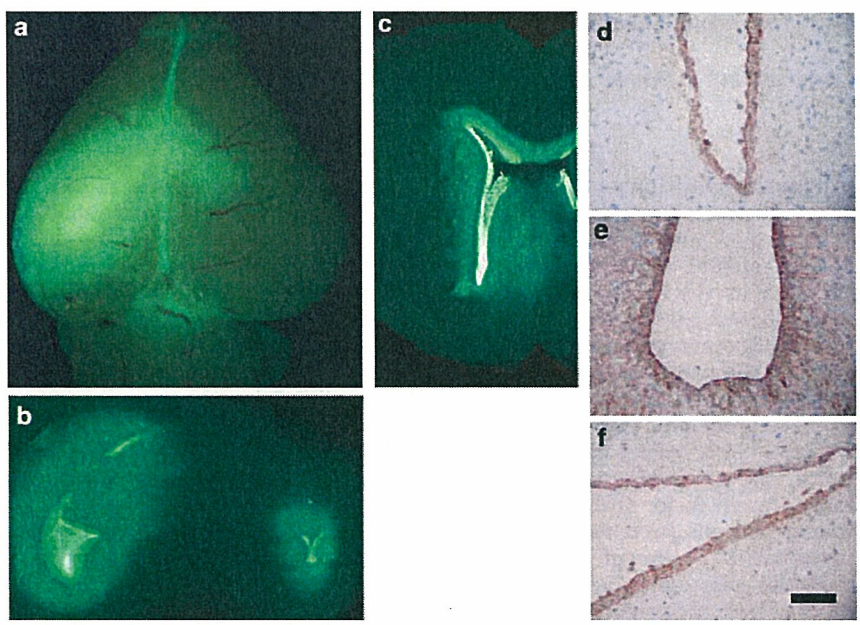

Figure 1 *Identification of cell types supporting SeV replication. SeV vector carrying GFP gene (SeV/GFP; 5×10^6 PFU/head) was injected into the left lateral ventricle of gerbils as described previously,[27] and the GFP expression 4 days after the injection was observed under a stereoscopic fluorescence microscope (Leica, Germany) from the surface of the top of brain (a) and with coronal sections around the hippocampus (b) and lateral ventricle (c). For the coronal sections, the brain was sliced into 300-μm-thick slices with a microslicer (DTK-1000; Dosaka, Japan). Representative photographs of immunohistochemical staining for SeV are shown (d–f). The paraffin sections were pretreated with 0.3% H_2O_2 in PBS, followed by washing thrice. After blocking with 10% normal goat serum (NGS) in PBS for 1 h, the sections were incubated overnight at 4°C with a rabbit polyclonal antibody to SeV (anti-SeV)[28] in 3% NGS and 0.3% Triton X-100 in PBS. The sections were then washed and incubated for 1 h with biotinylated anti-rabbit IgG (Vector Laboratories, Burlingame, CA, USA), followed by incubation for 1 h with the reagents for avidin–biotin complex formation (Vector Laboratories). Immunopositive cells were visualized by reaction with 3,3′-diaminobenzidine tetrahydrochloride (DAB) (WAKO Pure Chmicals, Tokyo, Japan) and counterstained with hematoxylin. Scale bars = 100 μm. The ependymal cells along the (d) lateral ventricle, (e) third ventricle and (f) hippocampus were SeV positive.*

injection into the cortex of adenovirus (1×10^8 PFU/head) carrying the GDNF gene.[29]

We next examined the effects of the postischemic administration of SeV vectors on the delayed neuronal death of the hippocampal CA1 pyramidal cells induced by transient ischemia. It has been reported that the direct administration of the bcl-2 gene mediated by adeno-associated virus (AAV) into pyramidal neurons within 1 h after ischemic insult prevents the delayed neuronal death in gerbils.[30] However, direct injection of virus vectors into the cerebral parenchyma cells, especially in the hippocampus, is more invasive than intraventricular administration. Therefore, we selected a single intraventricular administration and utilized SeV-transduced ependymal cells to produce proteins from the genes carried by the vectors.[27] Accordingly, SeV/GDNF and SeV/NGF (5×10^6 PFU/head) were injected into the lateral ventricles of ischemic gerbils after 30 min of occlusion of the bilateral carotid arteries, and histopathological analysis was conducted 6 days after the injection. The effects of the above vectors were compared with those of SeV vectors carrying brain-derived neurotrophic factor (SeV/BDNF), insulin-like growth factor-1 (SeV/IGF-1) and vascular endothelial growth factor (SeV/VEGF). All the genes carried by the vectors have been reported to prevent neuronal degeneration after transient ischemia,[31–33] and for each SeV vector, vector-derived expression in infected cells was confirmed *in vitro* (data not shown). In sham-operated gerbils, surviving wheel-like nuclei were observed in the pyramidal cells in CA1 (Figure 3a). However, in gerbils treated with SeV/GFP, almost all of the pyramidal cells in the hippocampal CA1 region showed pyknotic degenerative nuclei in the pyramidal cells (Figure 3g). In contrast, treatment of gerbils with SeV/GDNF or SeV/NGF ameliorated the delayed neuronal death in the hippocampal CA1 pyramidal cells (Figure 3b, c). Treatment with SeV/BDNF also showed ameliorative effects (Figure 3d), but treatment with SeV/VEGF did not (Figure 3f). Treatment with SeV/IGF-1 showed ameliorative effects (Figure 3e) in only two gerbils among eight tested. For quantitative analysis, the number of surviving neurons/1-mm length in the hippocampal CA1 region was counted (Figure 4). Treatment with SeV/GDNF (180.8 ± 11.7 cells/mm) or SeV/NGF (142.4 ± 24.3 cells/mm) significantly prevented neuronal death as compared to treatment with SeV/GFP (10.7 ± 1.9 cells/mm) ($P < 0.01$). Treatment with SeV/BDNF (139.3 ± 29.7 cells/mm) also reduced the cell death of the neurons by about 70%. SeV/GDNF and SeV/NGF (and SeV/BDNF) proved to be better for the treatment of transient global ischemia than SeV vectors carrying genes for the other factors investigated here. As a way to confirm that the vector-derived growth factors actually increased and acted to prevent the neuronal death of the hippocampal CA1 pyramidal neurons, we measured the concentrations of both NGF and GDNF proteins in the hippocampus of 'ischemic' gerbils 4 days after the injection of SeV/GDNF or SeV/NGF into the lateral ventricle. When the SeV/GDNF was injected at 4 h after ishemia, the concentration of GDNF (71.9 ± 12.0 pg/mg tissue) was increased compared to that of SeV/GFP-injected (0.057 ± 0.022 g/mg tissue) or untreated (0.038 ± 0.042 pg/mg tissue) gerbils. However, the concentration of NGF (15.8 ± 0.9 pg/mg tissue) remained at the original level of SeV/GFP-injected (15.4 ± 4.6 pg/mg tissue) or untreated (18.2 ± 6.2 pg/mg tissue) gerbils. When the SeV/NGF was injected at 4 h after ischemia, the concentration of NGF (1570 ± 210 pg/mg tissue) but not that of GDNF (0.074 ± 0.047 pg/mg tissue) increased, and this NGF could show a neuroprotective effect. These results indicate that the vector-derived growth factors rather than the intrinsic ones increase and function to prevent the neuronal death.

To examine the effect of extending the time until the administration of SeV vectors after ischemic insult, which is important for practical use in clinical applications,

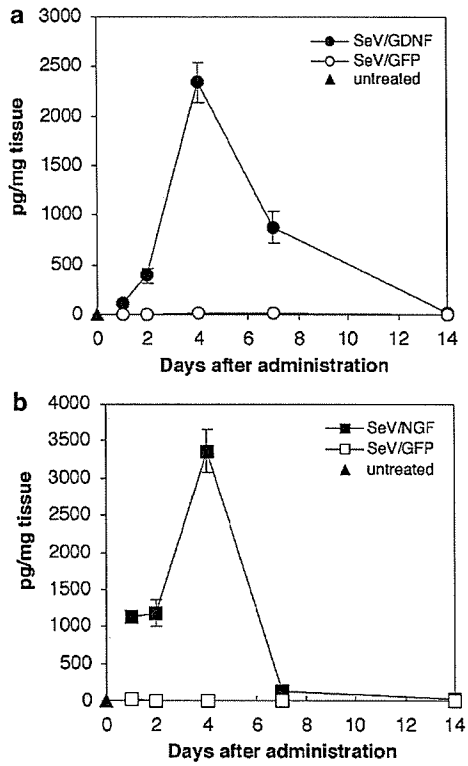

Figure 2 Kinetics of the expression of GDNF and NGF proteins in the hippocampus. Gerbils were injected with SeV vectors carrying GDNF (SeV/GDNF), NGF (SeV/NGF) or GFP (SeV/GFP) genes (5×10^6 PFU/head, n=20 animals per group) into the left lateral ventricle as described.[27] At 1, 2, 4, 7 or 14 days after the injection, the concentrations of GDNF and NGF in the hippocampus were measured using ELISA kits (Promega, WI, USA) as previously described.[27] The hippocampus was harvested from four gerbils at each time point. SeV/GDNF and SeV/GFP were constructed as previously described.[27] SeV/NGF was constructed as described.[27,28] Briefly, mouse NGF (accession number: M14805) cDNA was amplified with a pair of NotI*-tagged (underlined) primers containing SeV-specific transcriptional regulatory signal sequences, 5′-ACTTG CGGCCGCCAAAGTTCAGTAATGTCCATGTTGTTCTACACTCTG-3′ and 5′-ATCCGCGGCCGCGATGAACTTTCACCCTAAGTTTTTCTTA CTACGGTCAGCCTCTTCTTGTAGCCTTCCTGC-3′. The amplified fragment was introduced into the* NotI *site of the parental pSeV18$^+$b(+), +), which was constructed to produce the exact SeV full-length antigenomic RNA, to generate pSeV/NGF. pSeV/NGF was transfected into LLC-MK$_2$ cells after infection of the cells with vaccinia virus vTF7-3, which expresses T7 polymerase. The T7-driven full-length recombinant SeV/NGF RNA genomes were encapsulated by NP, P and L proteins, which were derived from the respective cotransfected plasmids. After incubation for 40 h, cell lysates of transfected cells were injected into embryonated chicken eggs to amplify the recovered viruses. The virus titers were determined using a hemagglutination units (HAU) assay. Values are expressed as the mean ± s.d.*